

NASA Contractor Report 2962

NASA  
CR  
2962  
c.1

TECH LIBRARY KAFB, NM



0061579

LOAN COPY: RETURN  
AFWL TECHNICAL LIBRARY  
KIRTLAND AFB, NM

# A Geometry Package for Generation of Input Data for a Three-Dimensional Potential-Flow Program

N. Douglas Halsey and John L. Hess

CONTRACT NAS1-14402  
JUNE 1978

**NASA**





## NASA Contractor Report 2962

# A Geometry Package for Generation of Input Data for a Three-Dimensional Potential-Flow Program

N. Douglas Halsey and John L. Hess  
*McDonnell Douglas Corporation*  
*Long Beach, California*

Prepared for  
Langley Research Center  
under Contract NAS1-14402



National Aeronautics  
and Space Administration

**Scientific and Technical  
Information Office**

1978



## 1.0 TABLE OF CONTENTS

1.0	Table of Contents . . . . .	iii
2.0	Index of Figures . . . . .	v
3.0	Summary . . . . .	1
4.0	Introduction . . . . .	2
5.0	Symbols . . . . .	7
6.0	Nomenclature and Arrangement of Input Points . . . . .	9
7.0	Paneling of Isolated Components . . . . .	13
7.1	General Features of the Paneling Method . . . . .	13
7.2	Distribution of Points Along N-lines . . . . .	17
7.2.1	Input Distribution, Unaltered . . . . .	17
7.2.2	Input Distribution, Augmented in Number . . . . .	18
7.2.3	Constant Increments in Arc Length . . . . .	20
7.2.4	Cosine Spacing. . . . .	20
7.2.5	Curvature-Dependent Distribution . . . . .	22
7.2.6	User-Specified Distribution . . . . .	24
7.3	Distribution of N-lines . . . . .	24
7.3.1	The Planar-Section Mode . . . . .	25
7.3.2	The Arc-Length Mode . . . . .	31
8.0	Calculation of Intersection Curves . . . . .	32
8.1	General Features of the Method . . . . .	32
8.2	Restrictions and Limitations of the Method . . . . .	32
8.3	Details of the Method of Solution . . . . .	33
8.3.1	The Initial Search for M-Line Segments and Surface Elements Containing Intersection Points . . . . .	34
8.3.2	The Final Search for M-line Segments and Surface Elements Containing Intersection Points and the Approximate Determination of the Intersection Points . . . . .	35
8.3.3	Derivation of a Mathematical Representation of the Surface of an Element . . . . .	37
8.3.4	Computation of More Precise Values of the Coordinates of the Intersection Points . . . . .	42
8.3.5	Test Cases for the Intersection Method . . . . .	43
9.0	Final Repaneling of Components. . . . .	47
9.1	General Considerations . . . . .	47
9.2	Intersecting Components . . . . .	48
9.3	Nonlifting Intersected Components . . . . .	51
9.4	Lifting Intersected Components . . . . .	54

10.0 Conclusions . . . . .	61
11.0 References . . . . .	62

## 2.0 INDEX OF FIGURES

1.	Typical element distribution for a trapezoidal wing . . . . .	3
2.	Typical element distribution for a wing-fuselage case . . . . .	3
3.	Surface elements used by NLR, Amsterdam, for an external store configuration (1780 elements) . . . . .	4
4.	Definition of frequently used terms . . . . .	9
5.	Illustration of numerical differentiation procedure . . . . .	15
6.	Comparison of curve-fit methods . . . . .	16
7.	Method of distributing points on an N-line — input distribution, augmented . . . . .	19
8.	Point distribution on a supercritical wing section — input distribution, augmented . . . . .	19
9.	Point distribution on a cylindrical fuselage section — constant increments in arc-length . . . . .	20
10.	Method of distributing points on an N-line — cosine distribution . . .	21
11.	Point distribution on a supercritical wing section — cosine distribution . . . . .	22
12.	Point distribution on a supercritical wing section — curvature-dependent distribution . . . . .	24
13.	Point distribution on a section of a nonlifting component — curvature-dependent distribution . . . . .	24
14.	Redistribution of elements on a trapezoidal wing (cosine spacing chordwise, constant increments spanwise, planar-section mode) . . . . .	28
15.	Redistribution of elements on a supercritical wing (cosine spacing chordwise, constant increments spanwise, planar-section mode, multisection component option) . . . . .	29
16.	Redistribution of elements on a fuselage (constant increments around circumference and in axial direction, planar-section mode, multi-section-component option) . . . . .	30
17.	Comparison of planar-section and arc-length modes of distributing N-lines — strut on a thick wing . . . . .	31
18.	Intersection method test case — intersection of two circular cylinders . . . . .	44

19.	Intersection method test case — intersection of two spheres . . . . .	45
20.	Intersection method test case — intersection of two ellipsoids . . . . .	45
21.	Illustration of intersection method — thick wing intersecting a circular cylinder . . . . .	46
22.	Final repaneling of intersecting components — wing-fuselage case . . .	49
23.	Final repaneling of intersecting components — wing-fuselage-tip-tank case . . . . .	50
24.	Final repaneling of nonlifting intersection components — wing-fuselage case (zero-incidence wing, N-lines through every point on intersection curve) . . . . .	55
25.	Final repaneling of nonlifting intersected components — wing-fuselage case (wing with $10^\circ$ incidence, N-lines through every point on inter- section curve) . . . . .	55
26.	Final repaneling of nonlifting intersected components — wing-fuselage case (zero-incidence wing, N-lines through every other point on intersection curve) . . . . .	56
27.	Final repaneling of lifting intersected components — wing-pylon case. .	57
28.	Final repaneling of lifting intersected components — wing-pylon case (sparse element distribution on pylon) . . . . .	58
29.	Final repaneling of lifting intersected components — wing-pylon case (more points on pylon than surrounding region on wing) . . . . .	59
30.	Final element distribution on a wing-fuselage-pylon case . . . . .	60

### 3.0 SUMMARY

The preparation of geometric data for input to three-dimensional potential-flow programs is a very tedious, time-consuming (and therefore expensive) task. This report describes a geometry package that automates and simplifies this task to a large degree. Input to the computer program for the geometry package consists of a very sparse set of coordinate data, often with an order of magnitude fewer points than required for the actual potential-flow calculations. Isolated components, such as wings, fuselages, etc. are paneled automatically, using one of several possible element distribution algorithms. Curves of intersection between components are calculated, using a hybrid curve-fit/surface-fit approach. Finally, intersecting components are rep paneled so that adjacent elements on either side of the intersection curves line up in a satisfactory manner for the potential-flow calculations. The geometry package has been incorporated into the NASA Langley version of the 3-D lifting potential-flow program and it is possible to run many cases completely (from input, through the geometry package, and through the flow calculations) without interruption. Use of this geometry package can significantly reduce the time and expense involved in making three-dimensional potential-flow calculations.



## 4.0 INTRODUCTION

With the advent of modern high-speed computers, the aerodynamicist gained the ability to study the effects of configuration changes in great detail. Whereas before he might have been able to estimate the effects of changes in such gross geometric parameters as sweep and aspect ratio on the total lift of an isolated wing, he now can accurately calculate the effects of changes of quite small details of the shape of very complex configurations (wing-fuselage-nacelle-pylon cases, for example) on not only lift but also on spanwise and chordwise load distributions, local pressures, flow angles, etc. This gain in computational ability has made the preparation of input data for describing configuration geometry a very tedious, time-consuming task. General three-dimensional potential-flow programs, such as the Hess program, (references 1 and 2) require the geometry to be input as the coordinates of sets of points, which are grouped to form quadrilateral surface elements. Many more elements are generally required to obtain accurate flow solutions than the number required for adequate pictorial representation. For example, the simple trapezoidal wing of figure 1, which can be represented fairly accurately by twenty or so elements, requires on the order of two hundred elements to obtain a reasonable flow solution. More complex configurations, such as the wing-fuselage case of figure 2, might use nearly a thousand. A case which was recently run by personnel of NLR, Amsterdam, using 1780 elements to represent an external-store configuration is shown in figure 3 (reference 3).

There is a clear need to automate as much as possible the preparation of the input coordinates, both in order to reduce the number of points input to the programs and in order to relax some of the restrictions on how the points must be distributed. The main difficulty in doing this is that there are so many logically different cases to consider. For example, a wing has different spacing requirements than a fuselage; a fuselage has different requirements than a nacelle, or a pylon, etc. Moreover, bodies of similar type may require different numbers and distributions of points due to the proximity of other bodies. If there are intersections between bodies, additional requirements are imposed on the point distributions. A geometry package must be very

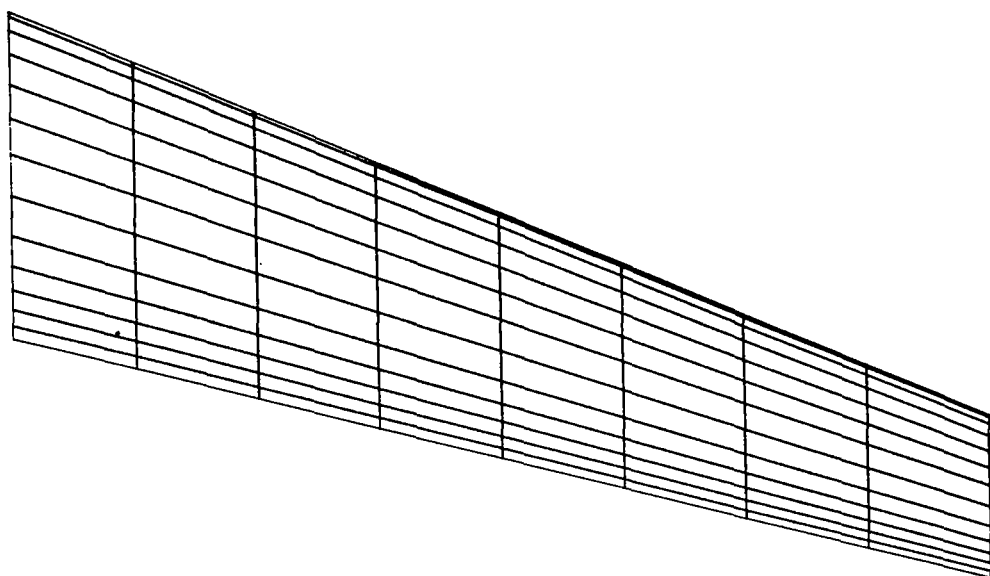


Figure 1. Typical element distribution for a trapezoidal wing.

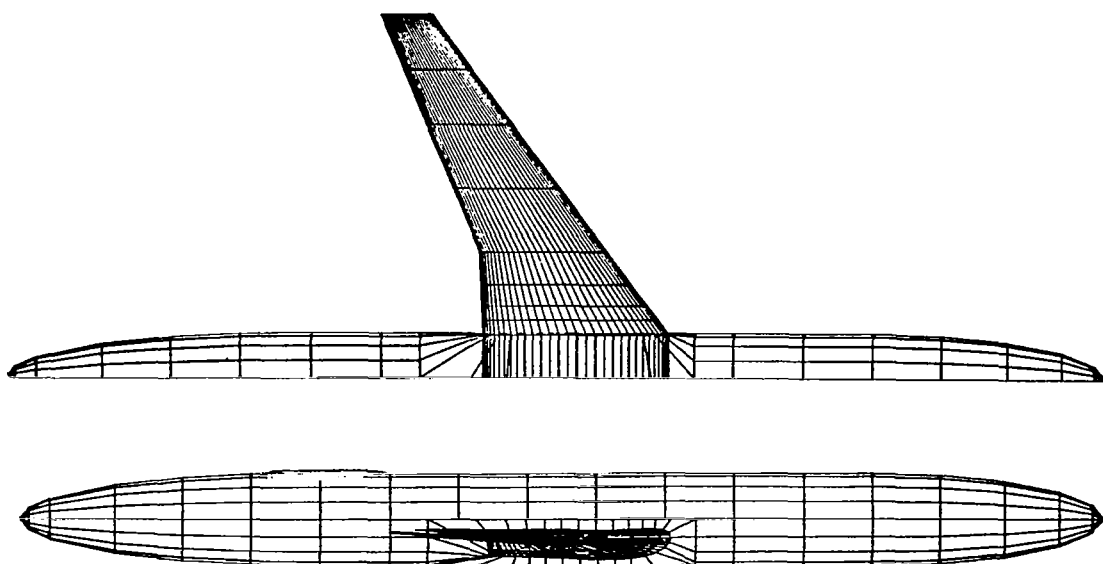


Figure 2. Typical element distribution for a wing-fuselage case.

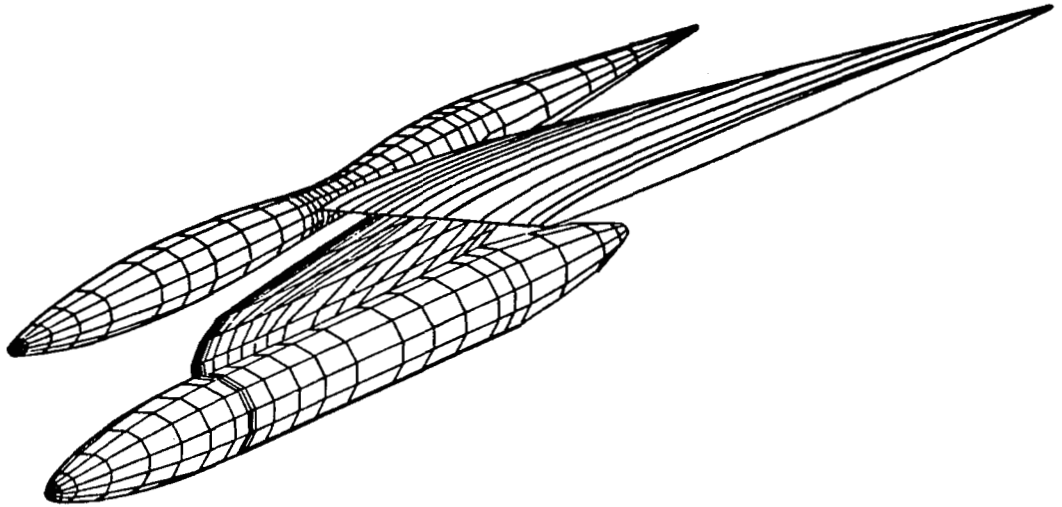


Figure 3. Surface elements used by NLR, Amsterdam, for an external store configuration (1780 elements).

very flexible to apply to so many different cases, but it should not be so flexible that it becomes cumbersome to use.

This report describes a geometry package developed for use with the potential-flow program of references 1 and 2 and for extensions of the method which may replace it in the future. Since the requirements of future programs are mostly speculative at the present, compatibility with the present program is emphasized.

The geometry package has been incorporated into the NASA-Langley version of the potential-flow program. This program accepts input either in the original input format described in reference 4 (with minor modifications) or in the format of the program described in reference 5. With a small amount of additional input to control the geometry package, it is possible to run a number of frequently occurring cases completely without human intervention. For example, isolated wings or bodies may be input to the program with a minimum number of points and the geometry package will augment and redistribute the points to the number and distribution specified by the user. These coordinates can then be punched on cards for use with automatic plotting programs to inspect the results before proceeding, or the potential-flow

program can proceed immediately to analyze the flow. Options are provided to allow the user to tailor the distributions to the needs of his particular problem, so it should also be possible to run cases having multiple non-intersecting wings or bodies with no human intervention. More difficult cases, involving intersecting components, can also be treated by the geometry package. Some of the simpler cases involving only two components, such as a wing/fuselage case, can also be run completely without intervention, but more complex cases almost certainly should be checked before proceeding with the flow calculation. Some cases cannot be completely handled by the geometry package, but in these cases, use of the geometry package to augment the point distributions and to calculate intersection curves still results in a significant reduction in the effort required to prepare the coordinate data. An outline of the major features of the geometry package is given below.

- o Significant reduction in effort required to input a case to the potential-flow program.
- o Two separate modes of program input available.
- o Complete compatibility with the potential-flow program — allowing many cases to be run completely without interruption between the geometry package calculations and the potential-flow calculations.
- o Paneling of isolated components
  - o Allows very sparse input coordinate data.
  - o Provides output coordinate data suitable for potential-flow analysis.
  - o Uses independent cubic curve-fits for interpolation in two directions on surfaces (N-lines and M-lines).
  - o Provides six options for the point distributions on N-lines and four options on M-lines.
  - o Allows all N-lines on a component to lie in parallel planes, if desired.
- o Calculation of intersection curves
  - o Requires a distinction between intersecting and intersected components.

- o Intersecting components represented by their M-lines only.
- o Intersected components represented by three-dimensional surface fits.
- o Intersection curves defined by arrays of intersection points between the M-lines of the intersecting components and the fitted surfaces of the intersected components.
- o Repaneling of intersecting and intersected components
  - o Intersection curve made an N-line of the intersecting component.
  - o Other N-lines on intersecting component shifted to restore a smooth distribution.
  - o Extra strip inside intersected component automatically generated, if desired.
  - o Intersected components repabeled to insure that elements on adjacent components line up along the intersection curves.
  - o Simpler repabeling options also provided.

The remainder of this report documents the theory and operation of the geometry package. Section 6 defines the geometric terms used in the later sections and discusses the basic philosophy of the geometric input to the method. Section 7 describes the paneling of isolated, non-intersecting components, including the options available, the applicability and limitations of the options, user requirements, methods used, and sample results. Section 8 covers the method of calculating curves of intersection between components, including the theory, restrictions, and verification cases. Finally, section 9 describes the methods that have been provided for repabeling components after having calculated the curves of intersection between them.

## 5.0 SYMBOLS

A	Matrix of surface-fit coefficients in algebraic form.
A,B,C,D	Coefficients of the equation of a plane.
A,B,C,D, E,F,G,H, I,J,K,L, M,N,O,P	Algebraic surface-fit coefficients.
c	Local value of the chord of a component.
d	Straight-line distance between adjacent points on a curve. Also used for the distance from a point to a plane.
F	Functions used to express a cubic curve in terms of the functional values and first derivatives at the ends of the curve only.
f	Dummy variable used to express the general form of a function used with several different variables.
G	Matrix of surface-fit coefficients in geometric form.
i	General subscript used in a variety of ways.
K	Parameter used in specifying the distribution of N-lines on a component.
k	Curvature at a point on a curve.
$\ell$	Subscript denoting variables associated with a line or curve.
M	Matrix of constants used in converting surface-fit coefficients from geometric to algebraic form.
M-line	Curve on a component, generally running spanwise on lifting components and in the axial direction on nonlifting components.
N	Total number of defining points on a curve.
N-line	Curve on a component, generally running chordwise on lifting components and in the circumferential direction on nonlifting components.
P	Total arc length of a curve.
$p_i$	Normalized point number of the point having index i.
S	Arc length along a curve.

$S_0, S_1$	Arc lengths at beginning and end of a curve.
$s$	Subscript denoting a surface.
$T$	Superscript denoting the transpose of a matrix.
$u, w$	Parameters used in calculating surface fits.
$x, y, z$	Coordinates of a point in a Cartesian coordinate system. Also subscripts referring to these coordinates.
$\beta$	Angle around a circle circumscribed about an airfoil section, used in determining the cosine point spacing distribution.
$\theta_i$	Angle of a curve at the defining point having index $i$ .
$\theta_{mi}$	Angle of a straight-line segment of a curve beginning at the defining point having index $i$ .

## 6.0 NOMENCLATURE AND ARRANGEMENT OF INPUT POINTS

Before describing the geometry package itself, it is necessary to discuss the general scheme for inputting points and for ordering the elements that they form and to define some of the terms which are used frequently throughout the remainder of the report. Most procedures and definitions are identical to those described in references 1 and 2, but some (for example, the definition of "ignored elements") have been changed slightly. Reference should be made to figure 4 to clarify the discussion which follows.

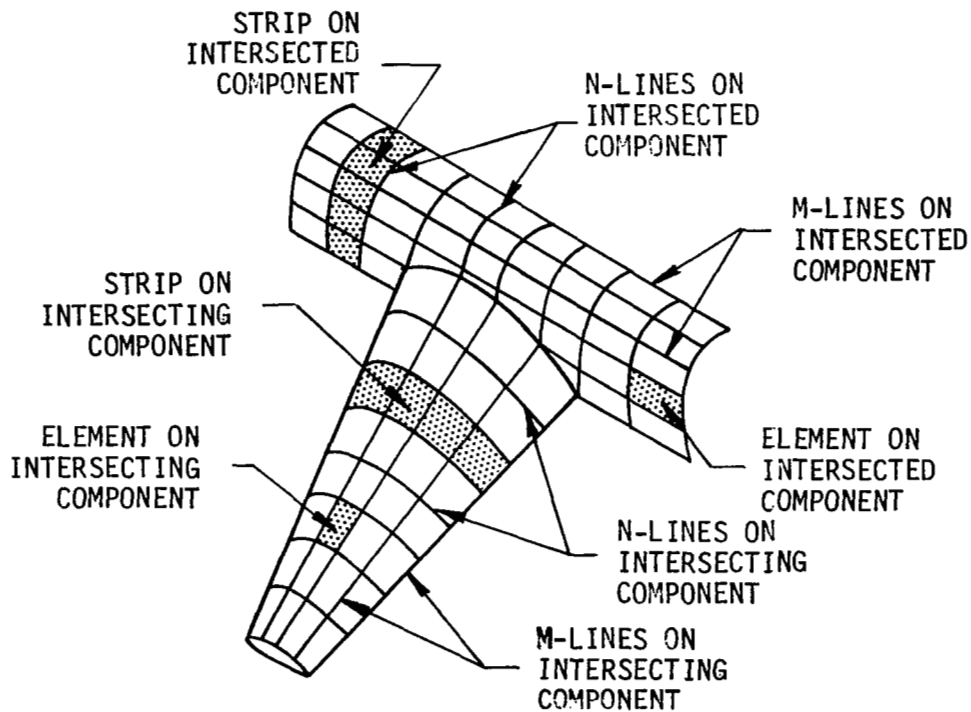


Figure 4. Definition of frequently used terms.



A complete configuration (such as a wing-fuselage-nacelle-pylon case) is assumed to be constructed of a number of components, each of which is a set of associated points. Normally a single component is used to represent a complete body (such as a wing or a fuselage), but any number of components per body is allowed. There are two types of components — nonlifting and lifting. Nonlifting components, such as fuselages or other blunt-ended bodies, are represented by source distributions over their surfaces and hence have no circulation. Lifting components, such as wings or other bodies with sharp trailing edges, are represented by both surface source and dipole distributions. Circulation about any section of a lifting component is adjusted in such a way as to satisfy the trailing-edge Kutta condition. Lifting components also have associated dipole sheets which represent trailing vortex wakes. Points on the wakes must be input to the program, as well as points on the bodies, and are considered to belong to the same components as the associated body points.

Each component consists of a set of points which can be connected in such a way as to form a network of intersecting lines called N-lines and M-lines. N-lines on lifting components are the lines running approximately in the chordwise direction. They divide a wing, for example, into a number of distinct sections. M-lines are the lines connecting corresponding points on the N-lines. On nonlifting components N-lines are generally those surrounding the major axis of the body (if it is possible to define an axis at all). In principle, the roles of the N-lines and M-lines on nonlifting components can be reversed without adversely affecting the execution of the program, but in most portions of the geometry package, it is assumed that the N-lines play the role described above. The potential-flow program does not require that all N-lines on nonlifting components have the same number of points. However since having variable numbers of points per N-line makes it impossible to define M-lines, most applications of the geometry package require each N-line to have the same number of points as each other N-line and each M-line to have the same number of points as each other M-line. N-lines may not cross other N-lines (though they may touch at a point); M-lines also may not cross other N-lines (though they may also touch at a point).

Points must be ordered so that all points on the first N-line (including wake points after the body points for lifting components) are input consecutively, followed by all points on the second N-line and so on. The first N-line input may be the one at either extreme of the component, but the choice determines the order of input of points along the N-lines. In general, the order must be such that the negative of the cross product of the vector from one point on an N-line to the next point on the N-line with the vector from a point on the N-line to the corresponding point on the next N-line results in a vector which is directed to the exterior of the component. This requirement may be satisfied on a wing, for example, by ordering the N-lines from tip to root and ordering points on the N-lines from the trailing edge along the lower surface to the leading edge and back along the upper surface to the trailing edge. On a fuselage the requirement is satisfied by arranging the N-lines from front to back and the points on each N-line increasing counterclockwise (looking aft). The requirement is also satisfied by reversing both the order of the N-lines and the order of the points on the N-lines. However parts of the geometry package require that N-lines on fuselages start at the front of the body, or more generally, that N-lines on nonlifting components start at the end farthest from the first M-line of any other components which intersect the component.

The area between adjacent N-lines on a component is designated a strip. Each strip on a lifting component has one characteristic value of the dipole distribution and one location where the Kutta condition is satisfied. On lifting components, it is possible to specify that a strip have a dipole distribution but no source distributions and no boundary conditions on any of its elements. Such a strip, called an extra strip, is useful for avoiding the abrupt ending of a dipole sheet (which would result in a concentrated vortex) along the curve of intersection of two components and for controlling the behavior of the dipole sheet near wing-tips when the piecewise linear vorticity option is used. Refer to reference 1 for more details.

The area (generally quadrilateral) between adjacent M-lines on a strip is termed an element. Each element has one control point where the boundary conditions are satisfied and one characteristic value of the source

distribution. It is possible to designate some elements to be ignored elements. These elements do not have source distributions and no boundary conditions are applied to them. If the component is lifting, ignored elements do have dipole distributions, however. References 1 and 2 allow for ignored elements to be defined only for lifting components, but this restriction has been lifted in the present program.

## 7.0 PANELING OF ISOLATED COMPONENTS

### 7.1 General Features of the Paneling Method

The first operation performed by the geometry package is to panel (i.e., distribute the elements) the components as isolated bodies, whether or not any of them intersect. Although the resulting element distributions on intersecting components may not be useful for analyzing complete configurations, they serve as a starting point for determining the final distributions as well as allowing a configuration "build-up" to be performed (i.e., the successive addition of components can be performed, in order to determine interference effects). It is assumed that each component is completely independent of all others. Since a single body may be composed of more than one component, however, and since the close proximity of another body may modify the element spacing requirements of a component, it is not always true that individual components are completely independent. Sufficient flexibility has been designed into the paneling method to allow points to be matched where components meet (making their M-lines continuous) and to allow the user to specify whatever distribution he deems appropriate to account for the proximity of other components.

The paneling of an individual component is accomplished in two steps. First the points on the initial N-lines are augmented in number and redistributed according to the number and the spacing algorithm specified by the user. For this calculation, the N-lines must be roughly chordwise on lifting components and, if the later repaneling of intersected components is required, the N-lines must be roughly circumferential about an axis on nonlifting components. Points in the wake of an N-line of a lifting component are distributed independently of the body points. Provision has been made to allow the user to input different numbers of points on the initial N-lines of a component. The process of redistributing points along the N-lines makes the numbers of points equal, thus allowing M-lines to be formed. The second step is to augment and redistribute the N-lines according to the number and algorithm specified by the user. This is done by augmenting and redistributing points along each M-line.

The process of redistributing points along either N-lines or M-lines requires a method of interpolating along general curves in space. Since these curves (particularly the N-lines) are not usually monotonic in either x,y, or z coordinates, some other parameter must be used as the independent variable of interpolation. In the present method, the parameter chosen is the arc length along the polygon formed by connecting straight-lines between adjacent points. In the remainder of this report the term "arc length" always refers to this straight-line approximation. Interpolation for a point on a curve requires three separate interpolations, one for each coordinate. Each separate interpolation is accomplished in two steps. In the first step, numerical differentiation of the dependent variable with respect to the arc-length is performed at each defining point on the curve. In the second step, the values of the function and its derivatives at the ends of the segments of the curve are used to derive the coefficients of cubic interpolating polynomials.

The numerical differentiation is done using a "weighted-angle" approach (see figure 5). In this approach, the lengths ( $d_i$ ) and angles ( $\theta_{m_i}$ ) of straight-line approximations to segments of the curve are first calculated. The angle at the midpoint of each segment is assumed to equal the angle of the straight-line approximation to the segment. The angle at any of the given points on the curve ( $\theta_i$ ) is then determined by taking an average of the angles of adjacent segments, weighted by the distances to the midpoints of the segments,

$$\theta_i = (d_i \theta_{m_{i-1}} + d_{i-1} \theta_{m_i}) / (d_i + d_{i-1}) \quad (7.1.1)$$

Angles of the first and last points on a curve are determined by extrapolation, assuming constant curvature between the first two and last two points. The derivatives at the given points are then found by taking the tangents of the calculated angles.

In order to facilitate the treatment of components having sections bounded by straight lines, such as a wing with a kink in its trailing edge or a fuselage with a cylindrical midsection, a multisection component option is provided in the numerical differentiation procedure. With this option,

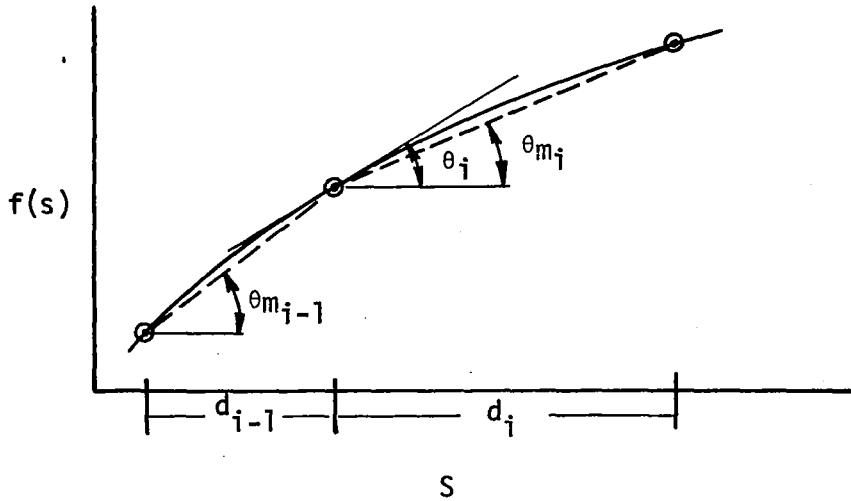


Figure 5. Illustration of numerical differentiation procedure.

the curve is divided into several sections. At the ends of the sections, extrapolations are used to determine the derivatives, just as they are at the ends of the complete curve. Sections consisting of just two points are represented by straight lines. The slopes of these straight lines then determine the derivatives at the ends of adjacent sections.

The values of the function and its derivative at each end of a curve segment constitute four pieces of information which can be used to determine the coefficients of a cubic polynomial approximating the curve. The form of the polynomial is

$$f(S) = f(S_0) + (S - S_0) f'(S_0) + \frac{1}{2}(S - S_0)^2 f''(S_0) + \frac{1}{6}(S - S_0)^3 f'''(S_0) \quad (7.1.2)$$

where  $S$  is the independent variable (arc length ranging from values  $S_0$  to  $S_1$ ),  $f$  represents the dependent variable ( $x$ ,  $y$ , or  $z$  coordinates), and primes denote differentiation. The form of its derivative is

$$f'(S) = f'(S_0) + (S - S_0) f''(S_0) + \frac{1}{2}(S - S_0)^2 f'''(S_0) \quad (7.1.3)$$

Given the values of  $f$  and  $f'$  at  $S_0$  and  $S_1$ , the simultaneous solution of equations (7.1.2) and (7.1.3) yields the values of  $f''(S_0)$  and  $f'''(S_0)$ . Equation (7.1.2) can then be used to determine the value of the function  $f(S)$  at any value of  $S$  within the given curve segment.

This curve-fit method does not insure continuity of the second derivative of the function and thus is not a cubic spline fit in the usual sense (reference 6). It was chosen rather than a spline method because of its consistently superior results in several test cases. For example, figure 6 shows a comparison between this method and a true cubic spline method. The interpolated coordinates found by the present method are considerably less wavy than those calculated using the spline method. Both methods fail to represent the shape accurately in the after region of the body, because of the higher local curvature and the proximity of the ends of the curve. Other comparisons involving airfoils and more general shapes also showed smoother results for the present method than the spline method, in

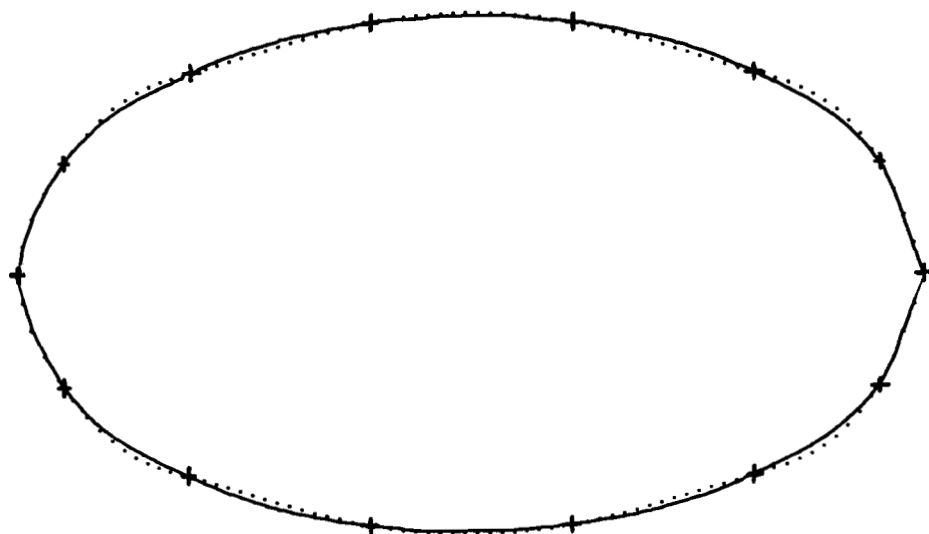
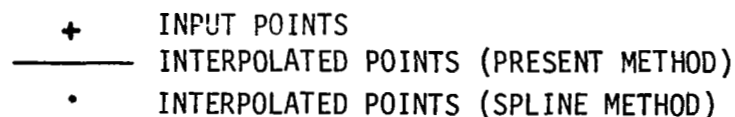


Figure 6. Comparison of curve-fit methods.

spite of the alleged proof in reference 6 that, in general, a spline produces the smoothest of all possible curve fits. The contradiction of this proof may possibly be due to the unusual character of the independent variable (it being defined as a quantity which varies smoothly along a nonsmooth curve) or it may be due to the presentation of the results by a graph of one interpolated result (the z-coordinates) as a function of other interpolated results (the x-coordinates).

## 7.2 Distribution of Points Along N-Lines

Each of the options for distributing points along N-lines (except the trivial option of leaving the initial distribution unchanged) requires an array of normalized arc lengths which applies to every N-line of the component under consideration. The formulas for these arc-length distributions are given below. Given the specified distributions, the method calculates the distribution on each initial N-line and interpolates each coordinate independently to determine the values at the desired locations. In some cases all points on an N-line coincide (as at the end of a pointed body, for example). Then the method does not attempt to interpolate, but simply provides the specified number of points to that N-line. The following options are available for distributing points on N-lines:

1. Input distribution, unaltered
2. Input distribution, augmented in number
3. Constant increments in arc length
4. Constant increments on the superscribed circle (cosine spacing)
5. Curvature-dependent distribution
6. User-specified distribution

### 7.2.1 Input Distribution, Unaltered

With this option the method does no interpolation. It should be used whenever the initial distribution already contains a sufficient number of properly spaced points. If the N-lines of the component under consideration are to be redistributed, or if the component is involved in an intersection with another component, then the number of points input must be the same on each component of the N-line. In addition, the distribution of points on adjacent



N-lines should be fairly similar so that when corresponding points on N-lines are connected, the resulting M-lines make smooth curves. This is the only option which may result in different numbers of points and different distributions of points among the N-lines of a component. Although no interpolations are required, some calculations are still necessary to determine the derivatives with respect to arc length of the coordinates at each point on each N-line. These are needed in later calculations to determine intersection curves.

#### 7.2.2 Input Distribution, Augmented in Number

This option results in a distribution which is similar to the initial distribution, but contains a different number of points. The initial distribution used in the calculation is the distribution for the first N-line on the component, unless all points coincide on the first N-line. In that case the distribution on the second N-line is used. The method works by defining a "normalized point number",  $p_i$ , ranging from zero to one,

$$p_i = (i - 1)/(N - 1) \quad (7.2.1)$$

where  $i$  is the index of the point and  $N$  is the total number of points. Arrays of normalized point number are formed for both input and output distributions. The output arc-length distribution is determined by interpolating the curve of input arc length versus input normalized point number to the output values of the normalized point number. This procedure is illustrated in figure 7. Suitable cases for this option include both lifting and non-lifting type components. It is especially useful for precisely controlling the desired distribution without having to load a large number of points and without having to determine in advance what the numerical values of the arc lengths are. Typical results for a section of a supercritical wing are shown in figure 8.

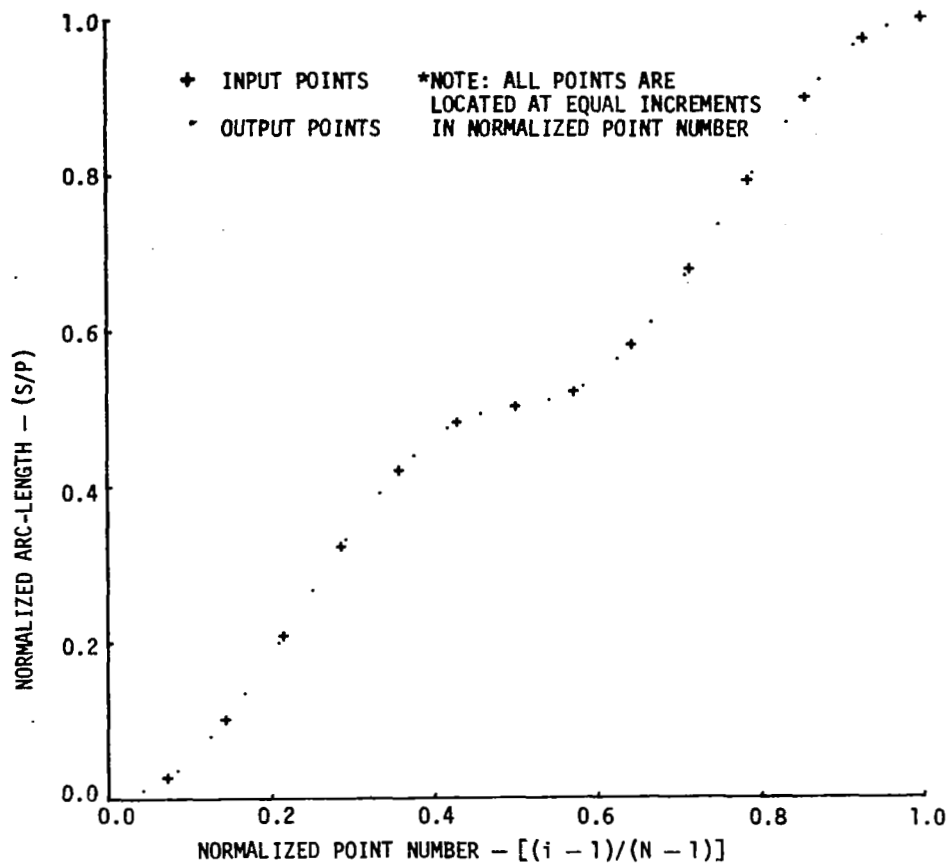


Figure 7. Method of distributing points on an N-line — input distribution augmented.

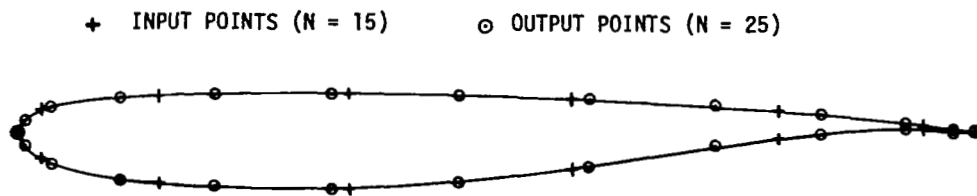


Figure 8. Point distribution on a supercritical wing section — input distribution, augmented.

### 7.2.3 Constant Increments in Arc Length

This option results in points distributed uniformly according to the formula

$$S_i/P = (i - 1)/(N - 1) \quad (7.2.2)$$

where  $S$  is the arc length measured from the first point and  $P$  is the total arc length around the perimeter of the  $N$ -line. It should be used for smooth bodies which do not have large variations in curvature (for example, the cylindrical fuselage section illustrated in figure 9. It should usually not be used for wing sections, since, for a reasonable number of points, there would be too few points to accurately define the shape near the leading edge or other high-curvature regions and too coarse spacing at the trailing edge for the Kutta condition to be accurately applied.

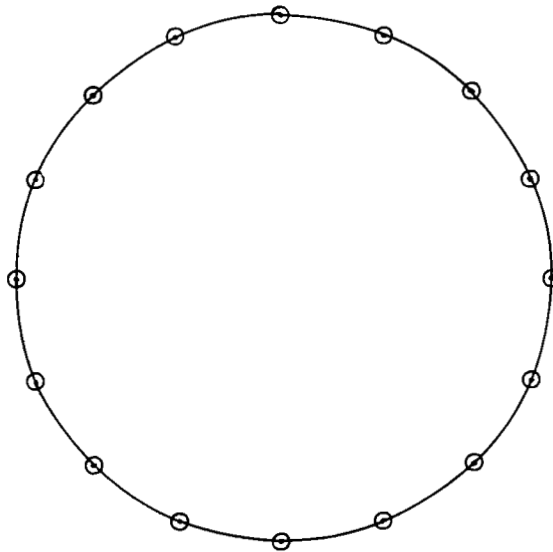


Figure 9. Point distribution on a cylindrical fuselage section — constant increments in arc length.

### 7.2.4 Cosine Spacing

Cosine spacing is a commonly-used distribution, dating from some of the classical two-dimensional theories (reference 7). Its name derives in an obvious way from the usual formula for the spacing

$$x_i/c = \frac{1}{2} \{1 + \cos[(i - 1)\pi/(N - 1)]\} \quad (7.2.3)$$

where  $c$  is the chord, which is assumed to be parallel to the  $x$ -axis. The significance of this method, as illustrated in figure 10, is that points are chosen having the  $x$ -coordinates corresponding to equal increments in angle around a circle circumscribed about the  $N$ -line with leading and trailing edges touching the circle. This results in very fine spacing near leading and trailing edges and coarse spacing in regions away from these edges. It is a useful distribution option for wing sections but would probably not be commonly used for nonlifting components.

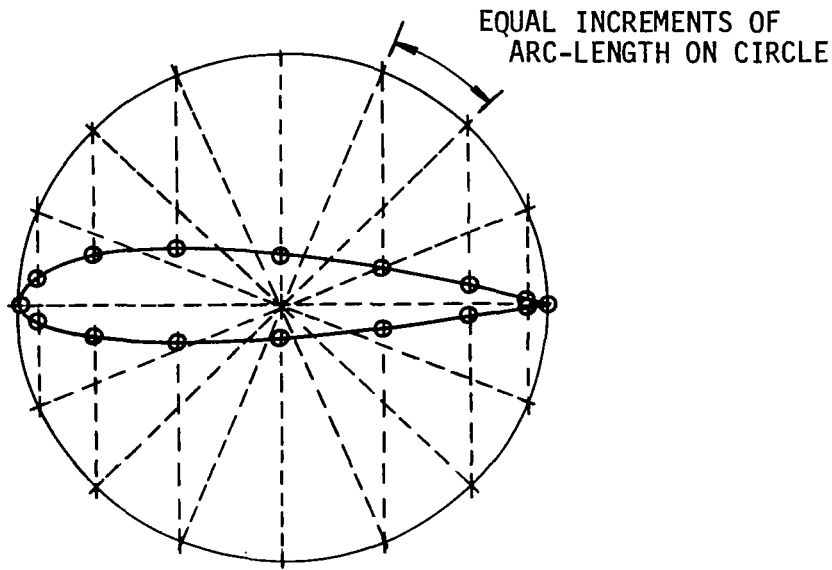


Figure 10. Method of distributing points on an  $N$ -line — cosine distribution.

Equation (7.2.3) is not directly useful for determining the specified arc-length distributions which the method of this geometry package requires. To do this, the wing section is first scaled to unit chord, translated to put the origin of the coordinate system at the leading edge, and rotated to make the chord parallel to the  $x$ -axis. The angle ( $\beta$ ) about the superscribed circle is then calculated for each point on the  $N$ -line by solving the equation

$$x_i/c = \frac{1}{2} (1 + \cos \beta) \quad (7.2.4)$$

using the transformed values of the x-coordinates. The arc-length distribution corresponding to the input points is also calculated. For both the angle and arc-length calculations, only the first N-line on a component is used (unless its length is zero, in which case the second one is used). Given the values of the arc-length distribution and the angle distribution for the input coordinates, and the desired values of the angle distribution for the output coordinates (uniform increments), the arc-length distribution for the output coordinates is determined by interpolation.

Results of this option for the same supercritical wing section used previously are shown in figure 11.

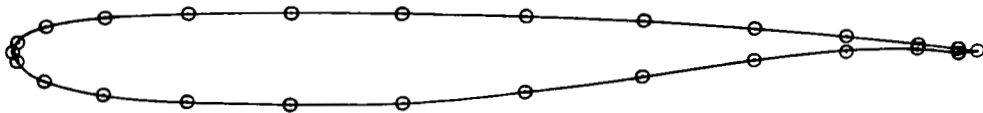


Figure 11. Point distribution on a supercritical wing section — cosine distribution.

#### 7.2.5 Curvature — Dependent Distribution

The accuracy and computational efficiency of the potential-flow method are both improved by using fine spacing in regions of high curvature and coarser spacing in regions of low curvature. This option produces a point distribution which depends on the curvature distribution along the first N-line of the component (or the second if the length of the first is zero). If the component is of lifting type, the point distribution is also made to be a function of the proximity to the trailing and leading edges in order to allow the trailing-edge Kutta condition to be accurately satisfied and to keep the variation of the spacing smooth in the leading-edge region where the curvature varies rapidly.

The following relationship between the curvature and the spacing increments is employed:

$$\Delta s_i = \{(1 - \Delta s_{\min}/\Delta s_{\max})(1 - k_i/k_{\max}) + \Delta s_{\min}/\Delta s_{\max}\} \Delta s_{\max} \quad (7.2.5)$$

where  $\Delta s_i$  is the  $i$ th increment in normalized arc length between adjacent points,  $k_i$  is the absolute value of the curvature at the center of the  $i$ th segment,  $k_{\max}$  is the maximum absolute value of the curvature on the N-line, and  $\Delta s_{\min}$  and  $\Delta s_{\max}$  are, respectively, the minimum and maximum allowable increments in arc length. In this application, the ratio  $\Delta s_{\min}/\Delta s_{\max}$  is specified to be 0.25.

To implement this relationship requires an iterative procedure. First the arc-length and curvature distributions are calculated. Then, if the component is of lifting type, the variable which plays the role of the curvature in equation (7.2.5) is modified to make its value at the trailing edge equal to its leading-edge value and to make it vary linearly from the leading and trailing-edge values to the values at 7.5 percent of the N-line's perimeter on either side of the leading and trailing-edge points. This modification insures that points will be closely spaced near the trailing edge and that the spacing will not vary abruptly near the leading and trailing edges. To start the iterations, estimates of the values of  $\Delta s_{\max}$  and all the values of  $\Delta s_i$  are required. These are all taken to be equal to the total length of the curve divided by the number of segments it contains. Given the estimated values of  $\Delta s_{\max}$  and  $\Delta s_i$ , the curvature at the center of each segment (modified as described above) is determined by interpolation of the curvature versus arc-length relationship and used in equation (7.2.5) to update the estimated values of  $\Delta s_i$ . These values are then scaled to make their sum equal to the total length of the N-line and searched to determine the value of  $\Delta s_{\max}$ . These updated values of  $\Delta s_i$  and  $\Delta s_{\max}$  are then used in the next iteration and the process is repeated a maximum of five times or until the required scale factor for the lengths of the increments is sufficiently close to unity.

Results of this option for the supercritical wing section used previously are shown in figure 12. Results for a section of a nonlifting component are shown in figure 13.

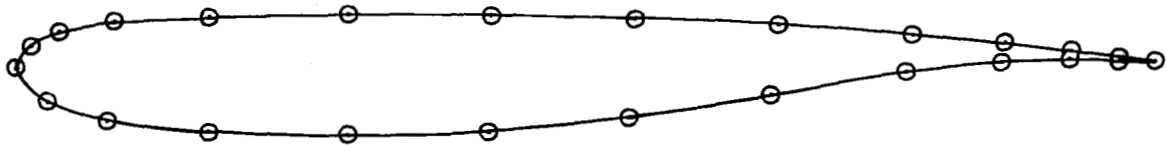


Figure 12. Point distribution on a supercritical wing section—curvature-dependent distribution.

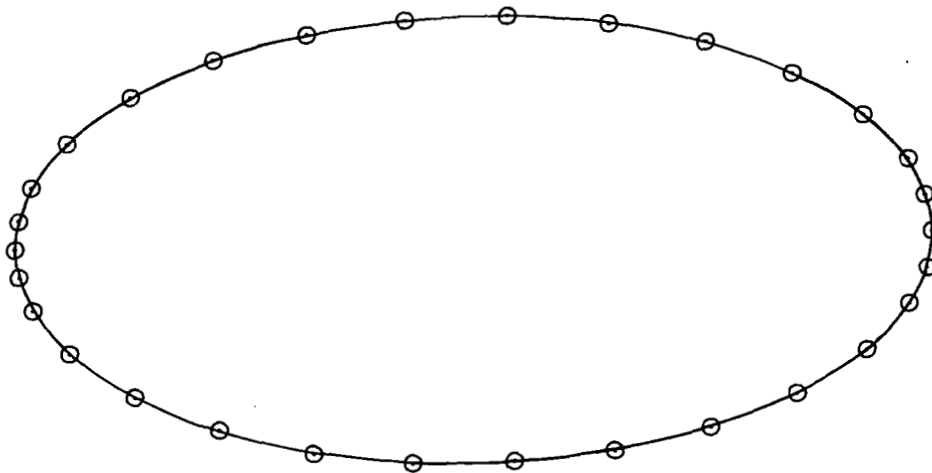


Figure 13. Point distribution on a section of a nonlifting component—curvature-dependent distribution.

#### 7.2.6 User-Specified Distribution

For N-lines of unusual shape or when components are located very close together, it is possible that none of the options described above will produce an adequate point distribution. To account for this possibility, provision has been made for the user to specify (as input data) values of the normalized arc lengths, which are used directly to determine the augmented coordinates.

### 7.3 Distribution of N-lines

After the points on the initial N-lines have been redistributed, each N-line on a component has the same number of points distributed in a similar manner. Connecting corresponding points on all N-lines generates a set of lines designated M-lines. Since the distribution of points is the same on each N-line, the M-lines are smooth and have fairly small curvature. The process of

augmenting and redistributing the N-lines is accomplished by augmenting and redistributing points along these M-lines. For these calculations, it is required that each M-line have a total length greater than zero.

There are four options available for the distribution of M-lines. They are:

1. Input distribution, unaltered
2. Input distribution, augmented in number
3. Constant increments
4. User-specified distribution

The descriptions of all four options are completely analogous to the descriptions of the corresponding options for distribution of points on N-lines described in section 7.2.

There are two modes of operation of this portion of the geometry package. The first (and most common) mode is designated the planar-section mode and the second is termed the arc-length mode in the discussions which follow.

#### 7.3.1 The Planar-Section Mode

The usual way of inputting data to the potential-flow program is to make the N-lines on a component planar cuts perpendicular to some axis of the component. For nonlifting components, this convention is just a convenience to the user. For lifting components, however, the elements are approximated by trapezoids, so that if the N-lines are not parallel, the accuracy of representation of the component by its elements is not as good.

The planar section mode of operation redistributes the points on the M-lines in such a way that all N-lines, except perhaps the first and last ones on a component, are parallel. The first and last N-lines generally define the planform view of the component, which is not required to be composed only of straight lines. The method does not alter these N-lines during this portion of the calculations. The distributions described above generally refer to the distances between the parallel planes, normalized by the distances between the first and last N-lines. At the edges of the component, when the first and last N-lines are not planar, the distributions refer to distances between the first



point on the N-line under consideration and the first point on the first N-line of the component, resolved in the direction perpendicular to the parallel planes and normalized by the distance between the first points on the first and last N-lines of the component. The orientation of the planes is defined by specifying (as input data) the direction cosines of a vector perpendicular to the planes. For this calculation, the sense of the normal vector is not important. However, if intersection curves are calculated and the components are subsequently repanelled, then the vector must point in the direction of increasing N-lines. If the direction cosines are not specified and the planar section mode is used, default values of (1.0, 0.0, 0.0) for nonlifting components and (0.0, -1.0, 0.0) for lifting components are assumed. When the default values are used, N-lines must be input from front to back on nonlifting components and from tip to root of lifting components.

The first step in distributing the points on the M-lines is to determine the equation of the planes representing the N-lines and the interpolating polynomials representing the M-line segments. The equations of the planes of the N-lines are of form

$$Ax + By + Cz + D_i = 0 \quad (7.3.1)$$

where A, B, and C are equal to the x, y, and z direction cosines of the vector normal to the planes (and hence are the same for all planes on the component). The values of  $D_i$  (different for each plane) are given by

$$D_i = D_1 + K_i(D_2 - D_1) \quad (7.3.2)$$

where  $D_1$  and  $D_2$  are the coefficients of the planes passing through the first and last points, respectively, on the first M-line of the component and  $K_i$  is the value of the distribution parameter for the N-line under consideration.  $D_1$  is determined from the relationship

$$D_1 = -(Ax_1 + By_1 + Cz_1) \quad (7.3.3)$$

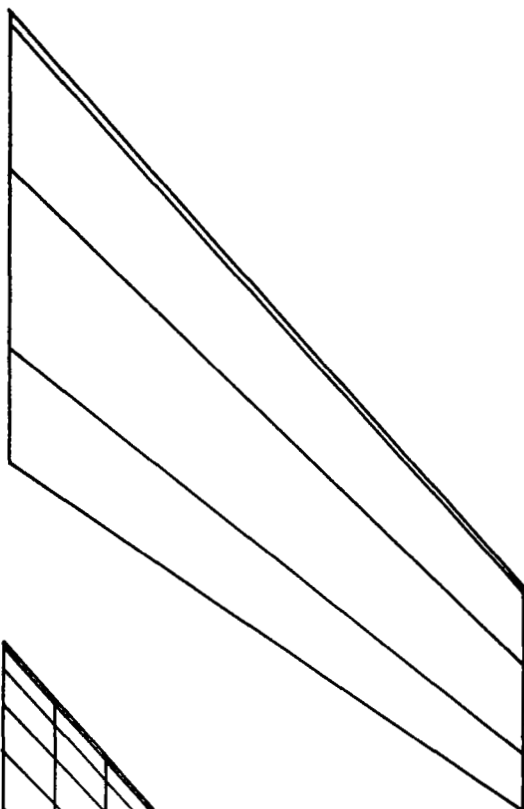
where  $x_1$ ,  $y_1$ , and  $z_1$  are the coordinates of the first point on the first M-line.  $D_2$  is determined in a similar manner, using the last point on the first M-line. The interpolating polynomials for the M-line segments are determined by the curve-fit procedure described in section 7.1.

The second step in distributing points on the M-lines is to determine which M-line segments intersect which planes. For this step, it is assumed that M-line curvature is small enough so that straight-line approximations to the M-line segments may be used.

Then, knowing which M-line segments intersect which planes and knowing the equations of the M-line segments and the planes, the coordinates of each intersection point can be computed. To do this for any point, substitute the expressions for  $x, y, z$  as a function of arc length along the M-line segment (each having the form of equation (7.1.2)) into the equation of the plane (7.3.1). This gives a single cubic equation with  $S_i$ , the arc length along the M-line segment to the intersection point, as the only unknown. This is solved by Newton's method. Using the intersection point of the plane and the straight-line approximation to the M-line segment to determine the starting point, the method typically requires only three or four iterations to converge to an adequate solution.

Figures 14 and 15 show the top views of two typical wings both before and after redistributing the N-lines. Since the wing in figure 14 is trapezoidal in planform and has a linear twist distribution, only the N-lines at the tip and root are needed in the initial geometric representation. Since the initial representations of the tip and root sections are already planar and all M-lines are straight lines, the planar-section mode and the arc-length mode (described in the next section) produce identical results. A more general case, for which the two modes of operation should give very different results is shown in figure 15. In this case, the M-lines on the entire outboard half of the span are straight lines, but they are curved on the inboard portion. Therefore, the multisection component option described in section 7.1 is used, allowing the linear portion of the geometry to be represented using only two N-lines. Figure 16 shows the top view of a fuselage before and after redistributing the N-lines. This fuselage has a cylindrical midsection with semi-ellipsoidal sections fore and aft. Again, the multisection component option allows the linear portion to be represented using only two N-lines. In all three of these cases, the redistributed N-lines are equally spaced.

INITIAL ELEMENT  
DISTRIBUTION



ELEMENT DISTRIBUTION  
AFTER REPANELING

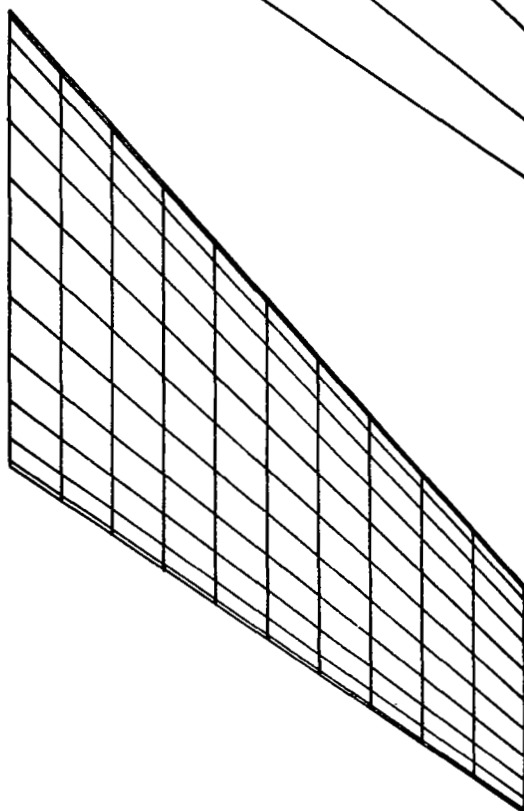
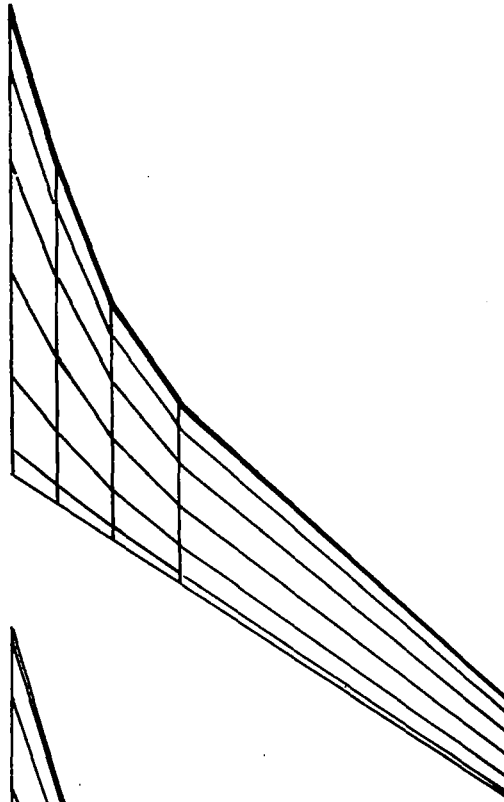


Figure 14. Redistribution of elements on a trapezoidal wing (cosine spacing chordwise, constant increments spanwise, planar-section mode).

INITIAL ELEMENT  
DISTRIBUTION



ELEMENT DISTRIBUTION  
AFTER REPANELING

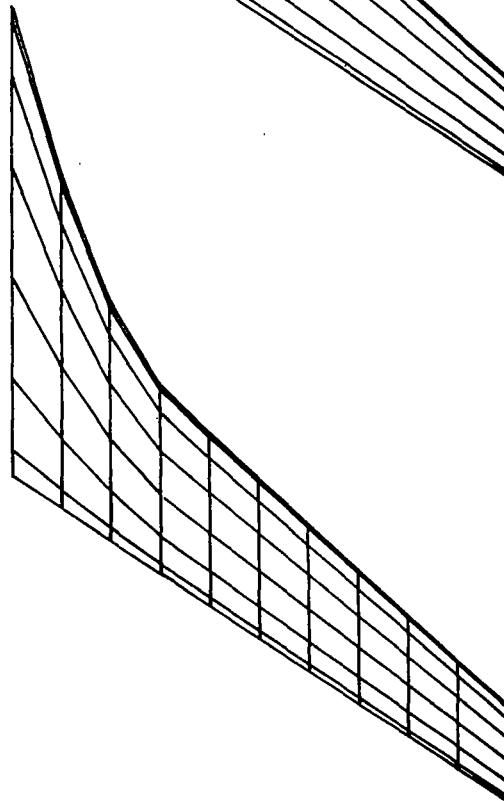
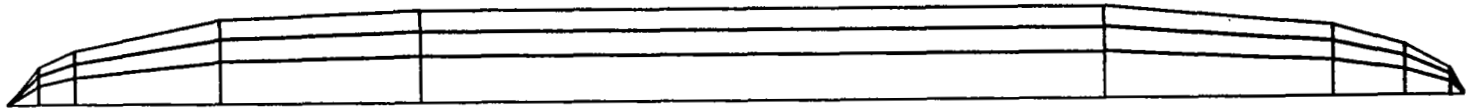


Figure 15. Redistribution of elements on a supercritical wing (cosine spacing chordwise, constant increments spanwise, planar-section mode, multisection component option).

## INITIAL ELEMENT DISTRIBUTION



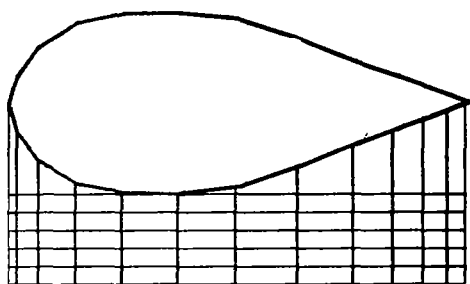
## ELEMENT DISTRIBUTION AFTER REPANELING



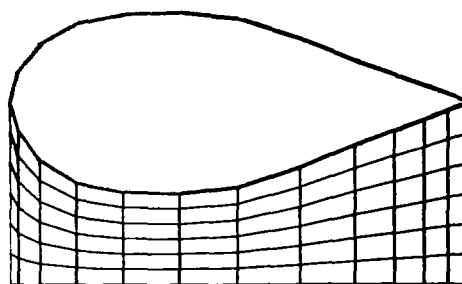
Figure 16. Redistribution of elements on a fuselage (constant increments around circumference and in axial direction, planar-section mode, multisection component option).

### 7.3.2 The Arc-Length Mode

In some cases the N-line at the edge of a component may be so highly nonplanar that a strip bounded by this N-line and an adjacent planar N-line would vary strongly in width, resulting in areas too sparsely covered with elements. An example of this is the under-wing pylon shown in figure 17(a). In this figure the thickness of the wing has been exaggerated to help illustrate the point. In such cases the arc-length mode of distributing N-lines on the component should be used. In this mode the specified distribution parameters refer to fractions of the total arc lengths of the M-lines, rather than to normalized distances between planes. The points on all M-lines of a component are distributed in a similar manner, so that the N-lines in the vicinity of the nonplanar edge of the component curve smoothly around to create a more uniform distribution of the elements, as illustrated in figure 17(b). In this mode of operation, the method of redistributing points along M-lines is completely analogous to the method of redistributing points along N-lines.



(a) Planar-Section Mode.



(b) Arc-Length Mode.

Figure 17. Comparison of planar-section and arc-length modes of distribution of N-lines — strut on a thick wing.

## 8.0 CALCULATION OF INTERSECTION CURVES

### 8.1 General Features of the Method

The second major operation performed by the geometry package is the calculation of the curves of intersection between body components. For this calculation it is assumed that the M-lines of one of the components (designated the intersecting component) pierce the surface of the other component (designated the intersected component). The final solution is a set of intersection points, one for each augmented M-line on the intersecting component. In general, the method calculates the intersection point of a curve and a surface and hence requires a surface-fit method as well as a curve-fit method. The surface-fit method uses the theory of parametric cubic surface patches originated by Coons (reference 8) and extensively developed and applied by a number of other investigators (reference 9, for example). The curve-fit method is the same one used in the paneling of isolated components and described in section 7.1.

### 8.2 Restrictions and Limitations of the Method

The intersection method is designed to handle cases which occur frequently in aircraft applications, such as wing-fuselage intersections, wing-pylon intersections, etc. It is not designed for complex cases in which the intersection curve is discontinuous or for cases involving fillets or smooth transitions from one component to the next. Use of the method is limited to cases in which the following restrictions apply:

1. A distinction can be made between intersecting and intersected components.
2. A component can intersect only one other component and can be intersected by only one other component. If a body intersects or is intersected by several bodies, it must be divided up into several components. A single component can intersect one component and be intersected by another component, however.
3. The M-lines on the intersecting component pierce the surface of the intersected component at a sharp angle. Surfaces are not tangent where they meet.

4. The M-lines on the intersecting component extend sufficiently far into the interior of the intersected component to allow a planar representation of the elements on the intersected component to be used in the process of searching for the elements which are intersected by the M-lines.
5. The intersecting component has at least one N-line which lies entirely in the interior of the intersected component.
6. No M-line on the intersecting component intersects the intersected component more than once.

### 8.3 Details of the Method of Solution

The method of calculation of the intersection curve between two components requires that one component be assigned the role of the intersecting component and the other component be assigned the role of the intersected component. This is done by the user in the input data to the geometry package. The intersection curve is then defined by the set of intersection points between the M-lines on the intersecting component and the elements on the intersected component. In order to define this curve at a sufficient number of points, every M-line on the intersecting component (after redistributing and augmenting the points on the N-lines) is used. On the intersected component, in principle either the original input elements or the elements after augmenting points on just the N-lines, or the elements after augmenting points on both N-lines and M-lines could be used for defining surface patches which are intersected by the M-lines of the intersecting component. Since parametric cubic surface patches are used, however, it is not necessary to use the large number of elements that exist after augmenting points on both N-lines and M-lines. Since the input points may vary in number from one N-line to the next, and since the distributions may also be dissimilar, use of the original input elements could result in surface patches having much more extreme curvature (and hence less accuracy) than use of either of the other two sets of elements. Therefore, the elements after augmenting points on the N-lines but before augmenting points on the M-lines are used for the formation of surface patches.

One possible method for calculating intersections of an M-line and a surface might operate as follows: Derive mathematical formulas to represent



each segment of the M-line and each element of the surface and find the roots of the equations obtained by equating coordinate values on the segments and the elements. If a particular equation has no real roots, or if it does have real roots but the points they represent fall outside the bounds of the element or the segment, then the element and the segment have no intersection points. If the equation does have real roots and the points they represent do fall within the bounds of both the element and the surface, then the roots are the intersection points. When all such equations have been solved, the intersection points are grouped, somehow, to determine the intersection curves. Such a method would have to solve a large number of equations (a number equal to the number of M-line segments multiplied by the number of surface elements) and many of these equations would fail to have solutions. It would, therefore, be very uneconomical to use.

A more economical approach, adopted in the present method, first compares maximum and minimum coordinate values on the M-line segments and the surface elements and eliminates from consideration those combinations which obviously contain no intersection points. Then an approximate intersection method, with planar element representations, is used to determine which M-line segments and surface elements contain intersection points and to get approximate values of the intersection point coordinates. Then, mathematical representations are obtained only for those elements containing intersection points, and these are used, together with the representations of the M-line segments, to calculate the intersection points more accurately. Details of this approach are given below.

### 8.3.1 The Initial Search for M-Line Segments and Surface Elements Containing Intersection Points

The basic information needed to conduct the initial stages of the search includes the maximum and minimum values of each coordinate on each element of the intersected component, on each strip of the intersected component, on each segment of the intersecting M-line, and on the entire intersecting M-line. Because it is assumed that the intersecting M-lines extend some distance into the body and a planar element representation can be used, it is legitimate to assume that the maximum and minimum values on an element must occur at one of its corners. A quick comparison of the coordinates of the corner points

thus determines the extrema. Extreme values on a strip are determined by comparing the extreme values of each of its elements. Values on the M-line segments are determined more accurately, assuming cubic relationships between the coordinate values and the straight-line arc lengths along the M-line (equations (7.1.2) and (7.1.3)). Equation (7.1.2) is set to zero (separately for  $x$ ,  $y$ , and  $z$ ) and solving gives two values of arc-length along the M-line (for each coordinate). The real solutions which fall within the bounds of the segment are used to calculate coordinate values which are compared, along with the values at the ends of the segment, to determine the extreme values. Maximum and minimum values on the entire intersecting M-line are determined by comparing the extreme values of each of its segments.

Having determined the extreme values of the coordinates on strips and elements of the intersected component and on segments and the entirety of the intersecting M-line, the searching procedure begins by comparing the extreme coordinate values on the first strip of the intersected component with the values for the entire M-line. If the range of any of the coordinate values on the strip fails to include at least part of the range of the values of the same coordinate on the M-line, then no intersection can possibly occur on that strip. Successive strips are compared with the M-line until one is found which may possibly contain the intersection point. Then each element on the strip is compared with the M-line until a possible intersected element is found. Then each segment on the intersecting M-line is compared with the element until a possible intersecting segment is found.

#### 8.3.2 The Final Search for M-Line Segments and Surface Elements Containing Intersection Points and the Approximate Determination of the Intersection Points

Having found an element on the intersected component and a segment of the intersecting M-line which share, at least partially, the ranges of their  $x$ ,  $y$ , and  $z$ -coordinates, a more careful check on whether or not they intersect is made. If the element is not already triangular, it is divided into two triangles by drawing one of the diagonals across the quadrilateral region. Each element is then represented by two planar, triangular subelements. The planar coefficients of each subelement are determined, starting from the general form of the equation of a plane

$$Ax + By + Cz + D = 0 \quad (8.3.1)$$

by first dividing through by  $D$  (illustrating that there are only three independent unknowns in equation (8.3.1)) and rearranging to get

$$A/Dx + B/Dy + C/Dz = -1 \quad (8.3.2)$$

and then substituting the coordinates of the corner points of the subelement into equation (8.3.2) to obtain a third-order system of linear equations which is easily solved for  $A/D$ ,  $B/D$ , and  $C/D$ .  $A$ ,  $B$ , and  $C$  are then found by multiplying by any arbitrarily chosen (finite, nonzero) value of  $D$ .

A check is then made to see if the ends of the M-line segment lie on opposite sides of the plane. This is done by computing the directed distance from each point to the plane, using the formula

$$d = \frac{Ax_1 + By_1 + Cz_1 + D}{\sqrt{A^2 + B^2 + C^2}} \quad (8.3.3)$$

where  $d$  is the distance and  $(x_1, y_1, z_1)$  are the coordinates of the point. If the value of  $d$  has the same sign for both end points, the segment does not intersect the plane of the triangular subelement. If this is true for both subelements on the element, the element and the M-line segment do not intersect and the next segment is considered.

When an M-line segment which does cross the plane of one of the subelements is found, the point of intersection of the segment and the plane is found using the method described in section 7.3.1. For this calculation, the M-line segment is again represented by a cubic polynomial. Given the intersection point, it is next necessary to check whether or not it falls within the triangular region of the subelement. To do this, the present method checks that each side of the triangle lies on the same side of both the intersection point and the opposite apex of the triangle. To determine that two points,  $A$  and  $B$ , lie on the same side of a line from points 1 to 2, the method takes the cross product of the vectors from  $A$  to 1 and from  $A$  to 2 and the cross product of the vectors from  $B$  to 1 and from  $B$  to 2 and checks whether or not the dot product of the two resulting vectors is positive.

If the point does not fall within the bounds of either triangular subelement, the next segment of the M-line is checked. If none of the segments intersects the element, the next element is checked in the above manner. If no element on the current strip contains the intersection point, the entire procedure, including the initial search described in section 8.3.1, is repeated for the next strip, and so on, until either an element of the intersected body and a segment of the intersecting M-line which contain the intersection point are found, or all possible combinations of elements and M-line segments are exhausted. If an approximate intersection point is found in this manner, it is used as a starting point for the iterative method described below, to determine a more precise intersection point. If the method fails to find an approximate intersection point, calculations continue, starting with the next M-line on the intersecting component. In this case, execution of the computer program is terminated after the intersection calculations since the final repaneling method requires the intersection curve to be uninterrupted and completely defined.

### 8.3.3 Derivation of a Mathematical Representation of the Surface of an Element

In order to compute a more accurate intersection point, it is necessary to obtain an equation for the surface of the element. This is done using the theory of parametric cubic surfaces described in references 8 and 9. The following discussion is a summary of relevant portions of the theory.

Required geometric quantities at each corner point of the element under consideration include the following (as well as the corresponding  $y$  and  $z$  values):

$$x, x_u, x_w, x_{uw}, x_{wu}$$

where the subscripts indicate differentiation and  $u$  and  $w$  are the parameters upon which the surface fit is based. On the boundary curves of an element,  $u$  represents a fraction of the straight-line arc length between the two M-line boundary curves and  $w$  represents a fraction of the straight-line arc length between the two N-line boundary curves. On the interior of an element,  $u$  and  $w$  represent quantities analogous to those defined above

but, for elements with compound curvature, the physical interpretation of the parameters is less obvious.  $x_u$  at a corner indicates the derivative of  $x$  with respect to straight-line arc length along the N-line passing through the corner, normalized by the straight-line distance between adjacent points on the N-line.  $x_w$  indicates the derivative with respect to straight-line arc length along the M-line passing through the corner, normalized by the straight-line distance between adjacent points on the M-line.  $x_{uw}$  and  $x_{wu}$  indicate cross derivative terms in the directions of the M-line and N-line. The first derivative terms (not normalized) were previously required for the calculations to redistribute and augment points along the M-lines and N-lines. They need only be normalized by the proper element side length to be applicable here. The cross derivative terms  $x_{uw}$  and  $x_{wu}$  are obtained by numerically differentiating the unnormalized first derivative terms along the M-lines and N-lines, respectively, and then normalizing by the product of the lengths of the adjacent element sides. The two cross-derivative values at each corner are then averaged, since the equation used to represent the surface implies that they are equal.

These geometric quantities, for  $x$ ,  $y$ , and  $z$  and for each corner of the element, constitute the so-called "parametric cubic patch coefficients in geometric form." The coefficients can be arranged in matrix form as follows (shown only for the  $x$  coordinates):

$$[G_x] = \begin{bmatrix} x_{00} & x_{01} & x_{w00} & x_{w01} \\ x_{10} & x_{11} & x_{w10} & x_{w11} \\ x_{u00} & x_{u01} & x_{uw00} & x_{uw01} \\ x_{u10} & x_{u11} & x_{uw10} & x_{uw11} \end{bmatrix} \quad (8.3.5)$$

In this matrix the  $u$  and  $w$  subscripts again represent derivatives as above. The 0 and 1 subscripts together indicate the corner of the element being considered, the first indicating the N-line and the second indicating the M-line. The 0 indicates the lower-numbered line on the element and the 1 indicates the higher-numbered line. Similar matrices are also formed for the  $y$  and  $z$ -coordinate terms.

The matrix of coefficients in geometric form,  $[G_x]$ , and the corresponding  $y$  and  $z$  matrices contain all the information needed to derive algebraic expressions for the coordinates at any point on the surface of the element in terms of the parametric variables. These expressions are of the following form (again shown only for the  $x$  coordinates):

$$\begin{aligned} x(u,w) = & w^3[A_x u^3 + B_x u^2 + C_x u + D_x] \\ & + w^2[E_x u^3 + F_x u^2 + G_x u + H_x] \\ & + w[I_x u^3 + J_x u^2 + K_x u + L_x] \\ & + [M_x u^3 + N_x u^2 + O_x u + P_x] \end{aligned} \quad (8.3.6)$$

The coefficients of equation (8.3.6) can be grouped to form the so-called "matrix of coefficients in algebraic form,"  $[A_x]$  as follows:

$$[A_x] = \begin{bmatrix} A_x & B_x & C_x & D_x \\ E_x & F_x & G_x & H_x \\ I_x & J_x & K_x & L_x \\ M_x & N_x & O_x & P_x \end{bmatrix} \quad (8.3.7)$$

To show how the matrix of coefficients in geometric form may be converted into the matrix of coefficients in algebraic form, it is first necessary to study the properties of equation (8.3.6) further. On the boundaries of the element one of the parametric variables is constant, either zero or one, and the other varies from zero to one. For definiteness, assume that the variable  $w$  is equal to zero. Equation (8.3.6) then reduces to a cubic equation with  $u$  as the only independent variable. On the opposite side of the element,  $w$  is equal to one and equation (8.3.6) reduces to another cubic equation, again with  $u$  as the only independent variable. The entire surface of the element can be considered to be a collection of cubic curves with  $w$  constant and  $u$  variable. Each of these curves has the form of equation (7.1.2), which can be converted to the form

$$f(u) = F_1(u)f(0) + F_2(u)f(1) + F_3(u)f'(0) + F_4(u)f'(1) \quad (8.3.8)$$

by solving for the second and third derivative terms in (7.1.2) as described in section 7.1. When this is done, the terms  $F_1(u)$ ,  $F_2(u)$ ,  $F_3(u)$ , and  $F_4(u)$  are given by

$$\begin{aligned} F_1(u) &= 2u^3 - 3u^2 + 1 \\ F_2(u) &= -2u^3 + 3u^2 \\ F_3(u) &= u^3 - 2u^2 + u \\ F_4(u) &= u^3 - u^2 \end{aligned} \quad (8.3.9)$$

or in matrix notation

$$[F] \equiv [F_1(u) \ F_2(u) \ F_3(u) \ F_4(u)] = [u^3 \ u^2 \ u \ 1] \cdot [M] \quad (8.3.10)$$

where

$$[M] = \begin{bmatrix} +2 & -2 & +1 & +1 \\ -3 & +3 & -2 & -1 \\ 0 & 0 & +1 & 0 \\ +1 & 0 & 0 & 0 \end{bmatrix} \quad (8.3.11)$$

In matrix notation, equation (8.3.8) becomes

$$\begin{aligned} F(u) &= [F] \cdot [f(0) \ f(1) \ f'(0) \ f'(1)]^T \\ &= [u^3 \ u^2 \ u \ 1] \cdot [M] \cdot [f(0) \ f(1) \ f'(0) \ f'(1)]^T \end{aligned} \quad (8.3.12)$$

where  $T$  indicates that the transpose of the matrix is to be taken. Now, using (8.3.12), the equations for  $x(u)$  and  $x_w(u)$  on the boundary curves  $w = 0$  and  $w = 1$  can be written as

$$\begin{aligned} x(u,0) &= [u^3 \ u^2 \ u \ 1] \cdot [M] \cdot [x_{00} \ x_{10} \ x_{u00} \ x_{u10}]^T \\ x(u,1) &= [u^3 \ u^2 \ u \ 1] \cdot [M] \cdot [x_{01} \ x_{11} \ x_{u01} \ x_{u11}]^T \\ x_w(u,0) &= [u^3 \ u^2 \ u \ 1] \cdot [M] \cdot [x_{w00} \ x_{w10} \ x_{uw00} \ x_{uw10}]^T \\ x_w(u,1) &= [u^3 \ u^2 \ u \ 1] \cdot [M] \cdot [x_{w01} \ x_{w11} \ x_{uw01} \ x_{uw11}]^T \end{aligned} \quad (8.3.13)$$

or more compactly

$$[x(u,0) \ x(u,1) \ x_w(u,0) \ x_w(u,1)] = [u^3 \ u^2 \ u \ 1] \cdot [M] \cdot [G_x] \quad (8.3.14)$$

Equation (8.3.12) can also be used to derive the expression

$$x(u,w) = [w^3 \ w^2 \ w \ 1] \cdot [M] \cdot [x(u,0) \ x(u,1) \ x_w(u,0) \ x_w(u,1)]^T \quad (8.3.15)$$

or equivalently

$$x(u,w) = [x(u,0) \ x(u,1) \ x_w(u,0) \ x_w(u,1)] \cdot [M]^T \cdot [w^3 \ w^2 \ w \ 1]^T \quad (8.3.16)$$

Combining (8.3.14) and (8.3.16) gives

$$x(u,w) = [u^3 \ u^2 \ u \ 1] \cdot [M] \cdot [G_x] \cdot [M]^T \cdot [w^3 \ w^2 \ w \ 1]^T \quad (8.3.17)$$

Since equation (8.3.6) can be rearranged and written as

$$x(u,w) = [u^3 \ u^2 \ u \ 1] \cdot [A_x] \cdot [w^3 \ w^2 \ w \ 1]^T \quad (8.3.18)$$

the matrix of coefficients in geometric form is converted to the matrix of coefficients in algebraic form by the operation

$$[A_x] = [M] \cdot [G_x] \cdot [M]^T \quad (8.3.19)$$

Expressions for the  $y$  and  $z$  coordinates as functions of the parameters  $u$  and  $w$  are obtained in a similar manner, using the matrices of geometric quantities  $[G_y]$  and  $[G_z]$ .

Including coefficients for all three coordinates, there are forty-eight parametric cubic quantities associated with each element. Except for the coordinates themselves (twelve of the forty-eight quantities), these quantities are generally not shared by adjacent elements. However, these coefficients are all derived from geometric data which is continuous from element to element and, therefore, is shared by adjoining elements. Therefore, a large reduction in the computer program storage requirements can be made, at a small expense of additional computation time, by storing all data in the (unnormalized) geometric form and converting to the algebraic form of equation (8.3.6) only when actually needed. Therefore, the coordinates, their derivatives along the  $N$ -lines, and  $M$ -lines, their cross-derivatives, and the arc



lengths between adjacent points are the only geometric data used in the present method.

#### 8.3.4 Computation of More Precise Values of the Coordinates of the Intersection Point

At this point, analytic expressions have been obtained for the coordinates along the intersecting M-line segment in terms of  $s$ , the arc length along the segment (equation (7.1.2)) and for the coordinates on the surface of the element in terms of the parametric variables  $u$  and  $w$  (equation (8.3.6)). Designating points on the surface by the subscript  $s$  and points on the M-line segment by the subscript  $\ell$ , expressions have been obtained for  $x_\ell(s)$ ,  $y_\ell(s)$ ,  $z_\ell(s)$ ,  $x_s(u,w)$ ,  $y_s(u,w)$ , and  $z_s(u,w)$ . At the intersection point

$$\begin{aligned}x_\ell(s) - x_s(u,w) &= 0 \\y_\ell(s) - y_s(u,w) &= 0 \\z_\ell(s) - z_s(u,w) &= 0\end{aligned}\tag{8.3.20}$$

Equation (8.3.20) represents a system of three simultaneous nonlinear equations in the three unknowns  $(u,w,s)$ .

The solution of this system of nonlinear equations requires an iterative procedure which must start from some estimate of the solution. An estimate of the solution, in terms of the coordinates of the intersection point  $(x_i, y_i, z_i)$  was obtained during the searching procedure to determine which M-line segment intersects which element of the intersected component. An estimate of  $s_i$ , the arc length along the M-line segment to the intersection point, was also obtained. The coordinate data must be used to determine estimates of the values of the  $u$  and  $w$  variables at the intersection point  $(u_i, w_i)$ . In the present method, the two planar subelements are converted into a single planar element and the values of  $u$  and  $w$  in the planar element are then determined. The planar element is formed from the three corner points defining the subelement in which the approximation to the intersection point is located and a fourth point obtained by rotating the other corner point of the original element about the line separating the two subelements until it lies in the plane of the other three points.

The parametric coefficients of a point in a planar element bounded by straight lines can be determined most easily by first noting that all coefficients of second- and third-order terms in equation (8.3.6) must vanish and then by finding the other four coefficients directly from the properties of the sides of the element. The result is that equation (8.3.6) reduces to

$$x(u,w) = x_{00} + (x_{10} - x_{00})u + (x_{01} - x_{00})w + (x_{11} - x_{10} - x_{01} + x_{00})uw \quad (8.3.21)$$

Equations for the  $y$  and  $z$  coordinates have similar form. Given the values of  $x, y$  and  $z$  at a point, equation (8.3.21) and the corresponding  $y$  and  $z$  equations constitute a system of three equations for the two unknowns ( $u$  and  $w$ ). The nonlinear term  $uw$  is eliminated from each equation and then one equation is added to each of the other two equations to result, finally, in a system of two independent linear equations for the two unknowns.

Given the estimate of the variables ( $s_i, u_i, w_i$ ) at the intersection point, Newton's method is used to solve the nonlinear system (8.3.20). The process generally takes only four or five iterations to converge to an error in the square-root of the sum of the squares of the variables of less than  $10^{-5}$  for a typical case. When solved,  $s_i$  can be used in equation (7.1.2) and the corresponding equations for  $y$  and  $z$  to obtain the coordinates of the intersection point. Alternatively,  $u_i$  and  $w_i$  could be used in (8.3.6) and the corresponding  $y$  and  $z$  equations.

### 8.3.5 Test Cases for the Intersection Method

In order to verify the accuracy of the present method, a number of test cases were run. These are not examples of realistic aircraft components, but they were chosen because their intersection curves can be analytically determined. Figure 18 shows a relatively simple case, the intersection of two circular cylinders. Using only four elements to represent each quadrant of each cylinder produces remarkably good results. There is no discernable difference between the theoretical and the calculated results (to the scale plotted). This is an especially accurate case for any method, since the intersecting M-lines are straight lines and the elements on the intersected

component have curvature in only one direction. A more difficult case, the intersection of two spheres, is shown in figure 19. This case tests the full capability of the intersection method. The intersecting M-line segments are circular arcs. The intersected elements have curvature in both directions and some of the intersected elements have zero-length sides (i.e., some elements are triangular). Nevertheless, the present method's results, using 250 elements on each sphere, are very accurate; the calculated intersection curve is only very slightly different from the theoretical one. Figure 20 shows the final test case, the intersection of two ellipsoids. Like the case of the two spheres, this case shows good results, using 250 elements per body. The method failed to find intersection points for the M-lines parallel to the x-axis in figure 20, since these M-lines meet the intersected component tangentially.

In order to illustrate the method for a configuration more typical of aircraft configurations, figure 21 is included. This shows a wing intersecting a cylindrical section similar to the midsection of a typical fuselage. To give the intersection curve more character, the thickness of the wing has been greatly exaggerated.

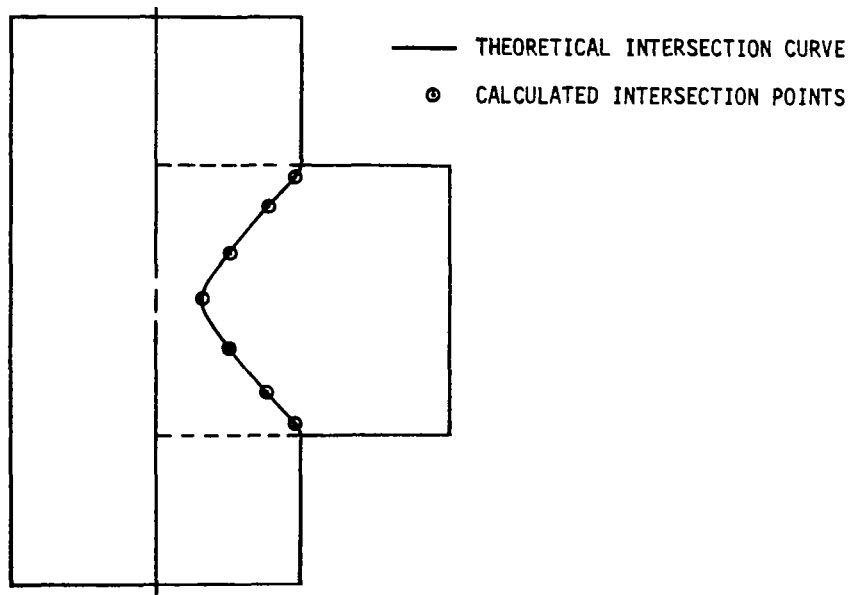


Figure 18. Intersection method test case — intersection of two circular cylinders (side view).

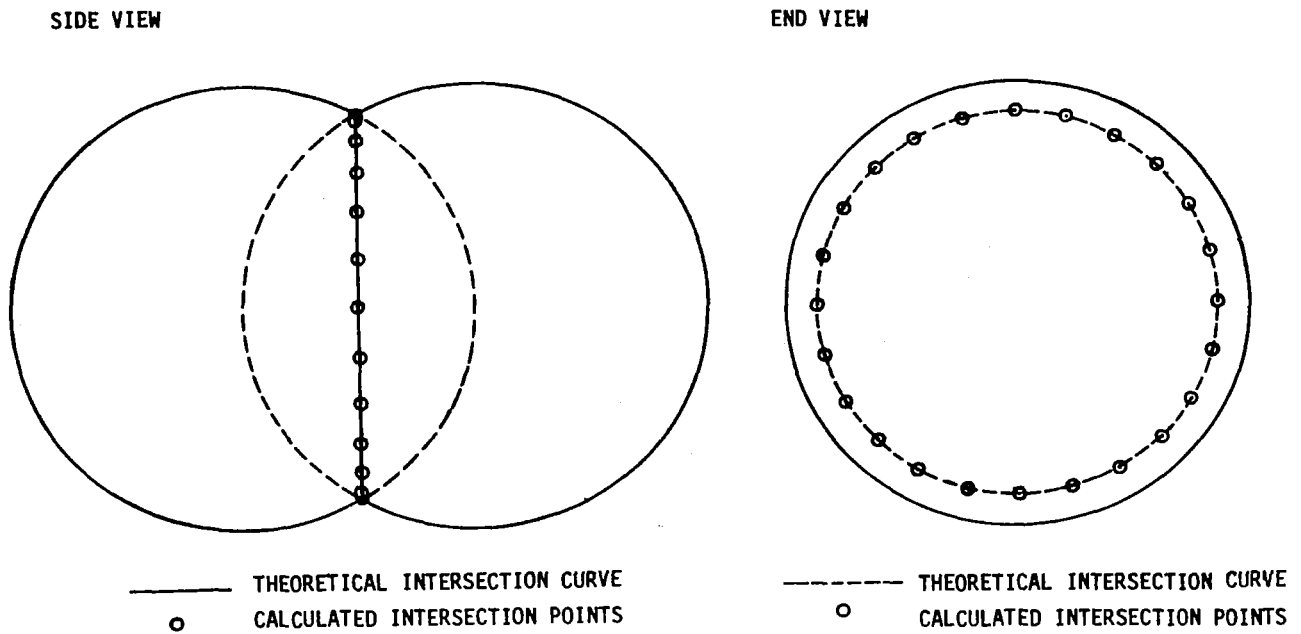


Figure 19. Intersection method test case — intersection of two spheres.

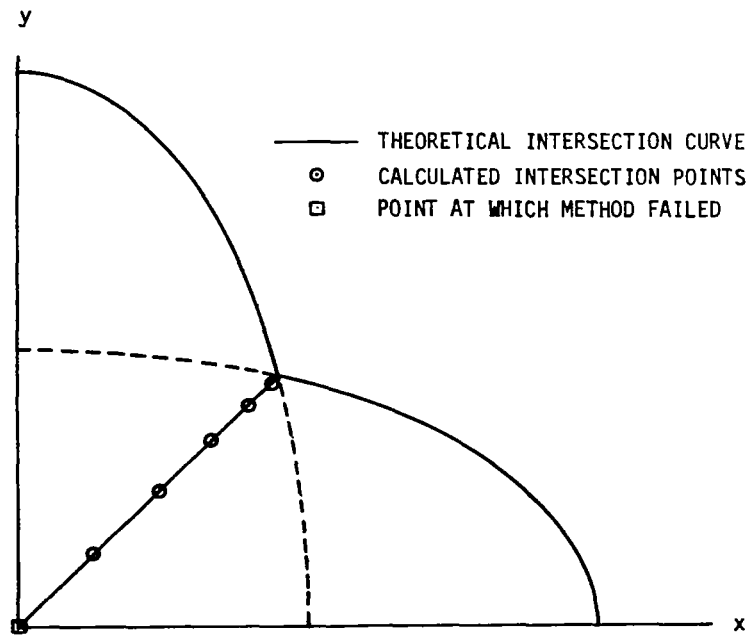
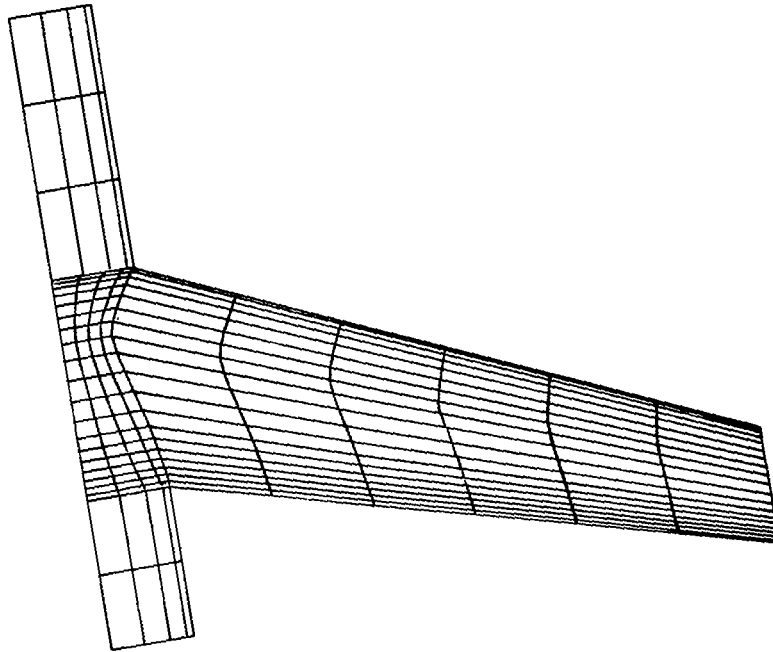


Figure 20. Intersection method test case — intersection of two ellipsoids (side view).

TOP VIEW



OBLIQUE VIEW

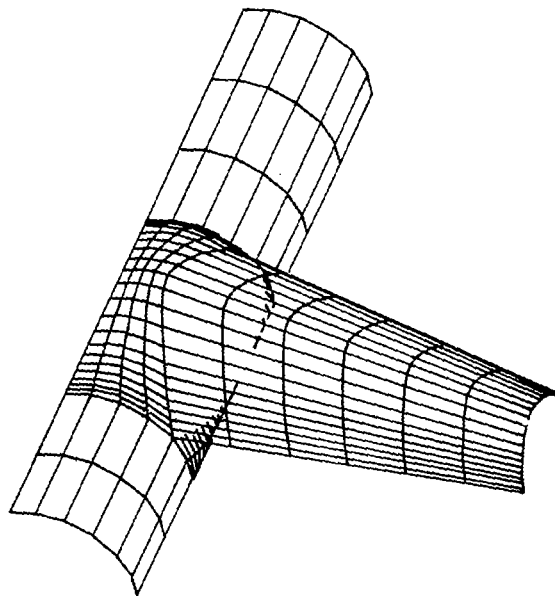


Figure 21. Illustration of intersection method — thick wing intersecting circular cylinder.

## 9.0 FINAL REPANELING OF COMPONENTS

### 9.1 General Considerations

The final major operation performed by the geometry package is the redistribution of points on all components which intersect other components. The point spacing requirements of the potential-flow method for intersecting bodies are not as well understood as those for isolated bodies. The accuracy of surface-singularity type methods in regions near concave corners is a matter of dispute in two-dimensions (reference 10) and has not been extensively studied in three dimensions. Some obvious requirements can be identified, however. One is that portions of components which fall inside other components should be eliminated, or in certain cases, designated as extra strips or ignored elements. Another is that the repaneling should not cause abrupt changes in the element spacing. Therefore, the entire component should be repaneled to produce a smooth transition from the paneling in the region of the intersection curve to the paneling in distant regions, rather than just the region of the intersection curve being repaneled. It is also possible that future potential-flow methods (such as the method of reference 5) will require the matching of the corners of the elements of adjacent components to eliminate or at least reduce the size of any gaps between elements.

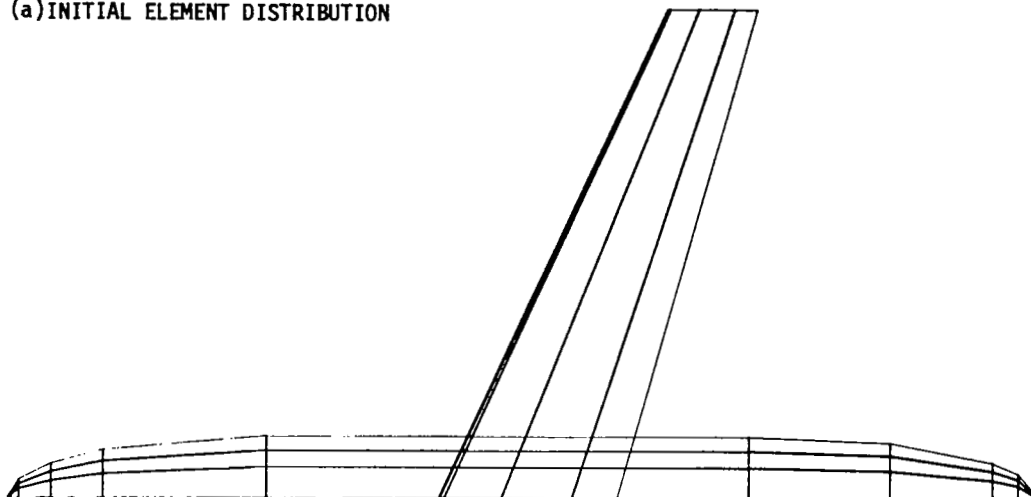
It is possible to envision innumerable different types of intersections between bodies, each of which would have its own special paneling requirements. It is not possible to develop a method sufficiently general to deal with them all. However, plausible paneling schemes can be developed for certain frequently occurring configurations, such as wing-fuselage or wing-pylon cases, so that these cases can be handled routinely. The present method divides all components which are involved in intersections into three distinct general categories and provides separate means of dealing with each of them. All intersecting components (those with M-lines which pierce other components) are repaneled one way, with only minor variations (whether they are lifting or nonlifting). Nonlifting intersected components are repaneled differently, and lifting intersected components are repaneled in a different way still. The methods used for these three categories are described in the following sections.

## 9.2 Intersecting Components

Typical examples of intersecting components include the wing in a wing-fuselage case, the pylon in a wing-ptyon case, the winglet in a wing-winglet case, etc. Although all these examples are of lifting intersecting components, they can also be nonlifting (struts, for example). Lifting and nonlifting intersecting components are repeneled in essentially the same manner. There is no redistribution of points along N-lines, only a redistribution of N-lines. In every case, a new N-line along the intersection curve is added. If the component is of lifting type and if the intersecting end of the component is designated as having an extra strip, then the entire area inside the intersected component (from the intersection curve to the end N-line) is made into a single strip by eliminating all intervening N-lines. If the component is of nonlifting type, or it does not have an extra strip at the intersecting end, then the portion inside the intersected component is simply eliminated. In the simplest cases, no other redistribution of points or N-lines is necessary. In most cases, however, the remaining N-lines on the exterior of the component must be moved in order to avoid irregularities in the widths of the strips. This is done by simply scaling the specified distances between N-lines by the fraction of the span of the component which lies outside the intersected component. To be more precise, the specified distances mentioned above are either the normalized distances between the planes of the N-lines (for the planar-section mode of operation) or the fraction of the arc lengths along the M-lines (for the arc-length mode of operation). The fraction of the span of the component which lies outside the intersected component is the fraction of the arc length along the M-line under consideration (for the arc-length mode of operation) or the fraction of the arc length along the first M-line of the component (for the planar-section mode of operation). The numerical techniques required to move the N-lines in this manner involve only interpolation procedures or cubic curve-plane intersection procedures which were described in section 7 above.

An example of the program capabilities for repeneeling intersecting components is shown in figure 22. Figure 22(a) shows a wing-fuselage case with the elements required for the initial geometric representation. In figure 22(b), the isolated components have been repeneeled, the intersection

(a) INITIAL ELEMENT DISTRIBUTION



(b) ELEMENT DISTRIBUTION  
AFTER FINAL RE PANELING OF WING

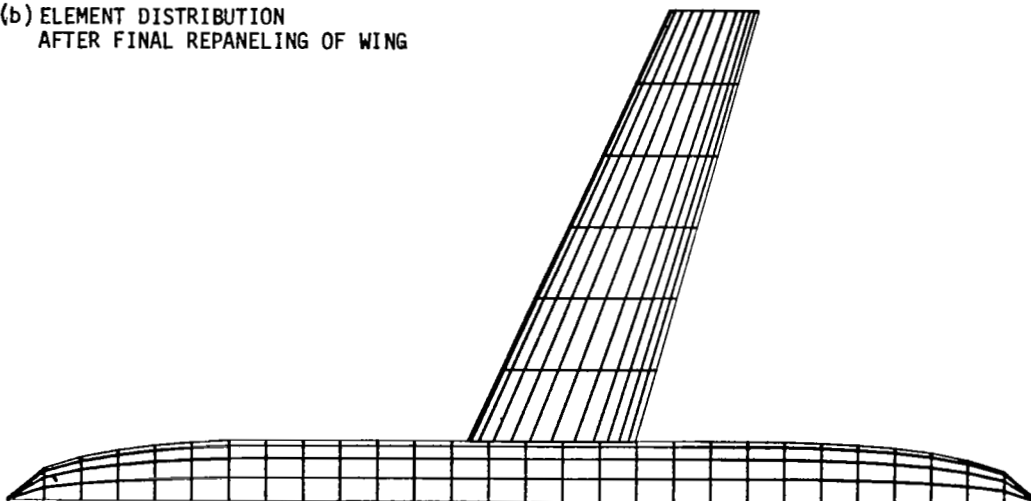


Figure 22. Final repaneling of intersecting components — wing-fuselage case.



curve has been made an N-line and all exterior N-lines have been redistributed to produce a smooth distribution. In addition, the area inside the intersected component has been made into an extra strip, but for clarity of presentation, the extra strip has not been shown in the figure.

More complicated cases, in which a body intersects more than one other body, can also be treated by this geometry package. However, in these cases, the intersecting body must be divided into more than one component. For example, in the case of the wing-fuselage with tip-tank shown in figure 23, the wing is divided (at fifty-percent semispan) into two components, an inboard component which intersects the fuselage and an outboard component which intersects the tip-tank. Since the same algorithm was used for distributing points on the N-lines of each component, and since points on the N-lines of intersecting components do not get redistributed, there is no mismatch in the elements at the junction between the components. Because of the redistribution of the N-lines, however, there is a small difference in the width of the strips in the inboard and outboard portions of the wing. Cases in which a body completely pierces several other bodies can be handled by dividing the intersecting body into components in an obvious way.

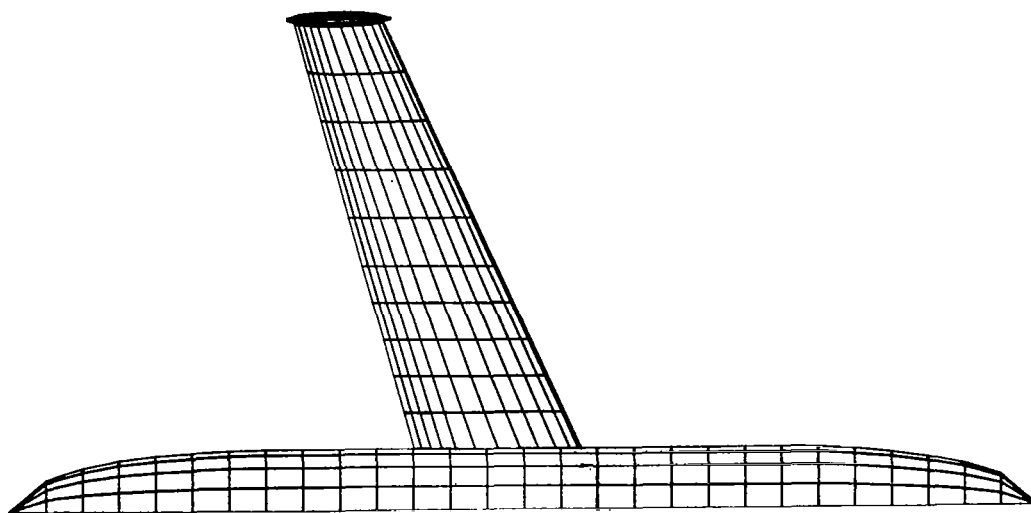


Figure 23. Final repaneling of intersecting components — wing-fuselage-tip-tank case.

### 9.3 Nonlifting Intersected Components

Typical examples of nonlifting intersected components include the fuselage in a wing-fuselage case, the tank in a wing-tip-tank case, etc. The most common application is to the wing-fuselage case. Therefore, the repaneling method in this geometry package was conceived primarily with fuselages in mind, but it should also be useful for other types of cases.

Three options are provided for the final repaneling of nonlifting intersected components. The simplest option is to do no repaneling at all, in which case the final element distributions are as shown in figures 22 and 23. If this option is used, a portion of the intersected component falls inside the intersecting component. If the intersecting component is not very thick, an adequate potential-flow solution may still be obtained in spite of this. If the intersecting component covers a significant area on the intersected component, then the elements inside the intersecting component should be designated ignored elements (elements with no singularities and no boundary conditions). Since there is no repaneling, however, some elements are only partially covered and the decision whether or not the elements should be ignored requires some user judgment. For this reason, no mechanism has been provided for automatically designating elements to be ignored elements on nonlifting intersected components. If the user desires to use ignored elements, he must repanel the configuration using the geometry package, punch the resulting coordinates on cards, and terminate execution of the program. Then he must execute the program a second time, using the punched output from the preceding case as input data, designating the ignored elements himself with the appropriate flags, skipping the geometry package, and proceeding straight to the potential-flow calculations.

With the first option, the element distribution on the intersected component is not influenced by the element distribution on the intersecting component. Experience with the method of references 1 and 2 indicates that there is no strong need to repanel fuselages in most wing-fuselage cases; accuracy of the potential-flow solution is usually adequate using a distribution of elements appropriate for an isolated fuselage case. However, in some cases even better accuracy is desired. Also the newer potential-flow methods, using surface doublet distributions, may require the elimination of the small gaps which result when the edges

of adjacent elements are not carefully aligned. The second and third options (both very similar) repanel nonlifting intersected components to produce element distributions which depend strongly on the element distributions on the intersecting components.

The calculations in both options start by defining a leading-edge and a trailing-edge point on the intersection curve. The trailing-edge point is assumed to be the first or last point on the intersection curve, since this curve is an N-line of the intersecting component and points on N-lines are input starting at the trailing edge, working around the perimeter, and ending back at the trailing edge. The leading-edge point is found by searching for the point on the intersection curve which has the smallest projected distance in the axial direction from the front of the intersected component. Because of this, nonlifting intersected components which are repaneled with one of these two options must be input starting at the upstream end, must have roughly streamwise M-lines, and must be paneled using the planar-section mode of operation. The axial direction is defined by the direction cosines of the vector perpendicular to the planes of the N-lines. Planar cuts are then made through the leading and trailing-edge points on the intersection curve, perpendicular to the axis of the intersected component. The points of intersection of these planes and the M-lines of the intersected component define new N-lines. All N-lines forward of the leading-edge point and all those aft of the trailing-edge point are then redistributed in a manner similar to the redistribution of the N-lines on intersecting components. Forward of the leading-edge point, this is done by scaling the projected distances in the axial direction from the front of the component by a factor equal to the ratio of the distance from the front of the component to the leading-edge point and the distance from the front of the component to the first N-line aft of the leading-edge point. Aft of the trailing-edge point, the redistribution is done the same way, except that the back of the component, the distance to the trailing-edge point and the distance to the first N-line in front of the trailing-edge point are used.

The two options differ only in the distribution of N-lines in the region between the leading and trailing-edge points on the intersection curve. One of the two options passes planar sections through each point on the intersection curve and uses the points of intersection of these planes and the

M-lines of the intersected component to define new N-lines. This option can be used when an element distribution with no gaps between adjacent elements is desired. The other option passes planar cuts through every second point on the intersection curve, starting with the leading-edge point and working aft on both upper and lower surfaces of the intersection curve. Since each surface may contain either an even or odd number of points, it is possible that planes will be passed through two consecutive points at the back of the intersection curve. This option can be used when gaps between adjacent elements can be tolerated, but it is desired to keep their size fairly small.

Having redistributed the N-lines, it is next necessary to redistribute the points on each N-line. The method for doing this is the same for both available options. First, a search of the N-line passing through the leading-edge point on the intersection curve is conducted to find the point closest (in arc length along the N-line) to the leading-edge point. This point is moved to coincide with the leading-edge point. The other points on this N-line are redistributed in a manner which makes the resulting arc-length distribution reasonably smooth and similar to the previous distribution. For points on the N-line before the point closest to the leading-edge point on the intersection curve, this is done by scaling the arc length along the N-line by a factor equal to the ratio of the arc length to the leading-edge point and the arc length to the point closest to the leading-edge point. For points on the N-line after the point closest to the leading-edge point, arc lengths are scaled the same way, but using arc lengths from the other end of the N-line. Having determined the arc-length distribution of the redistributed points, the coordinates are found by the same interpolation procedure described in section 7.1. Points are redistributed on N-lines forward of the leading-edge point using the same arc-length distribution as on the N-line which passes through this point. Between leading-edge and trailing-edge points, points on N-lines are redistributed in a similar manner by scaling the arc lengths by a factor determined from the ratio of the distances to the intersection point and to the point on the same M-line as the point closest to the leading-edge point. Aft of the trailing-edge point, points on all N-lines are redistributed using the same arc-length distribution as the redistributed points on the N-line passing through the trailing-edge point. Because the

N-lines through the intersection points between the leading- and trailing-edge points are broken by the intersection curve, it is necessary to break the component into more than one component. Presently, the program breaks the component into four smaller components, one forward of the leading-edge point, one below the intersection curve, one above the intersection curve, and one aft of the intersection curve.

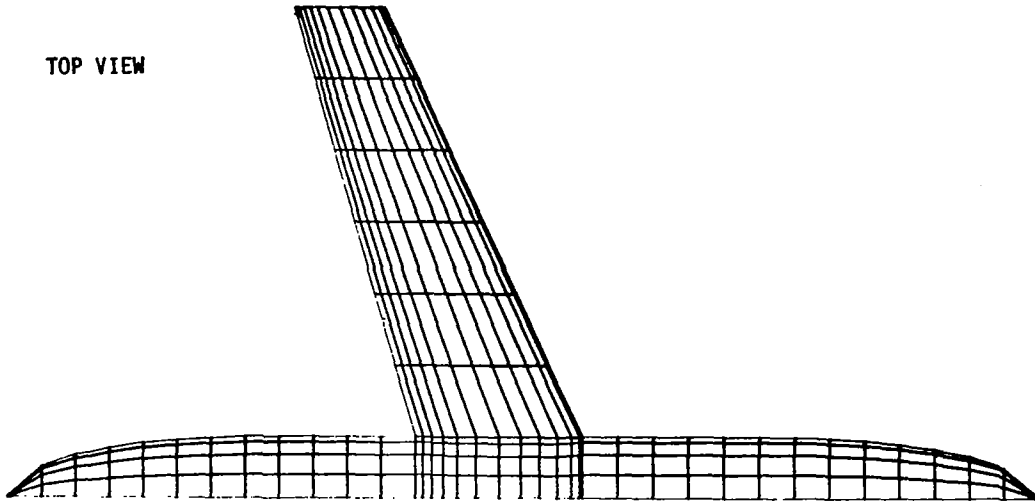
A typical example of the results of this repaneling method is shown in figure 24. This case shows a wing-fuselage with the wing at zero incidence, located slightly above the axis of the fuselage. In this case, use has been made of the option which passes an N-line through every point on the intersection curve. Figure 25 shows a similar case, using the same option. In this case, however, the wing has ten degrees of incidence, illustrating the point that, for such cases, the present method bunches points below the intersection curve and spreads them out above the intersection curve. In extreme cases, this may result in an unacceptable element distribution with many elements bunched tightly near the bottom of the component and very few elements near the top. However, most cases will probably be much less extreme than the one shown, for which the element distribution is adequate. Figure 26 shows a wing-fuselage case similar to the one of figure 24, but with the wing located at the same level as the axis of the fuselage. In this case, the option which passes N-lines through every second point on the intersection curve has been used.

#### 9.4 Lifting Intersected Components

The most common example of a lifting intersected component is the wing in a wing-pylon or wing-with-strut case.

As in the case of nonlifting intersected components, lifting components are treated three different ways. Again, the simplest option is to do no repaneling at all. In this case, part of the intersecting component covers a portion of the surface of the intersected component and the remarks of section 9.3 concerning accuracy of the solutions, the desirability of using ignored elements, and the mechanism for generating them again apply.

TOP VIEW



SIDE VIEW (fuselage only)

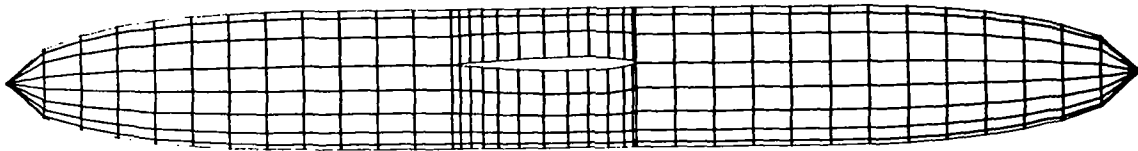


Figure 24. Final repaneling of nonlifting intersected components — wing-fuselage case (zero-incidence wing, N-lines through every point of intersection curve).

SIDE VIEW (fuselage only)

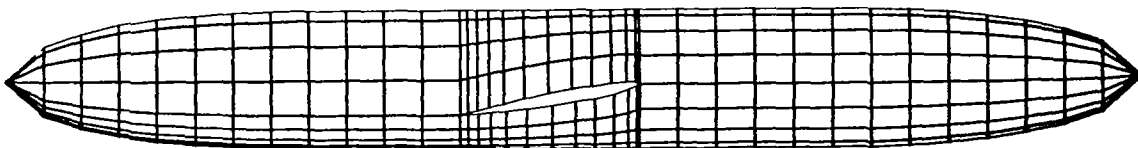


Figure 25. Final repaneling of nonlifting intersected components — wing-fuselage case (wing with  $10^\circ$  incidence, N-lines through every point on intersection curve).

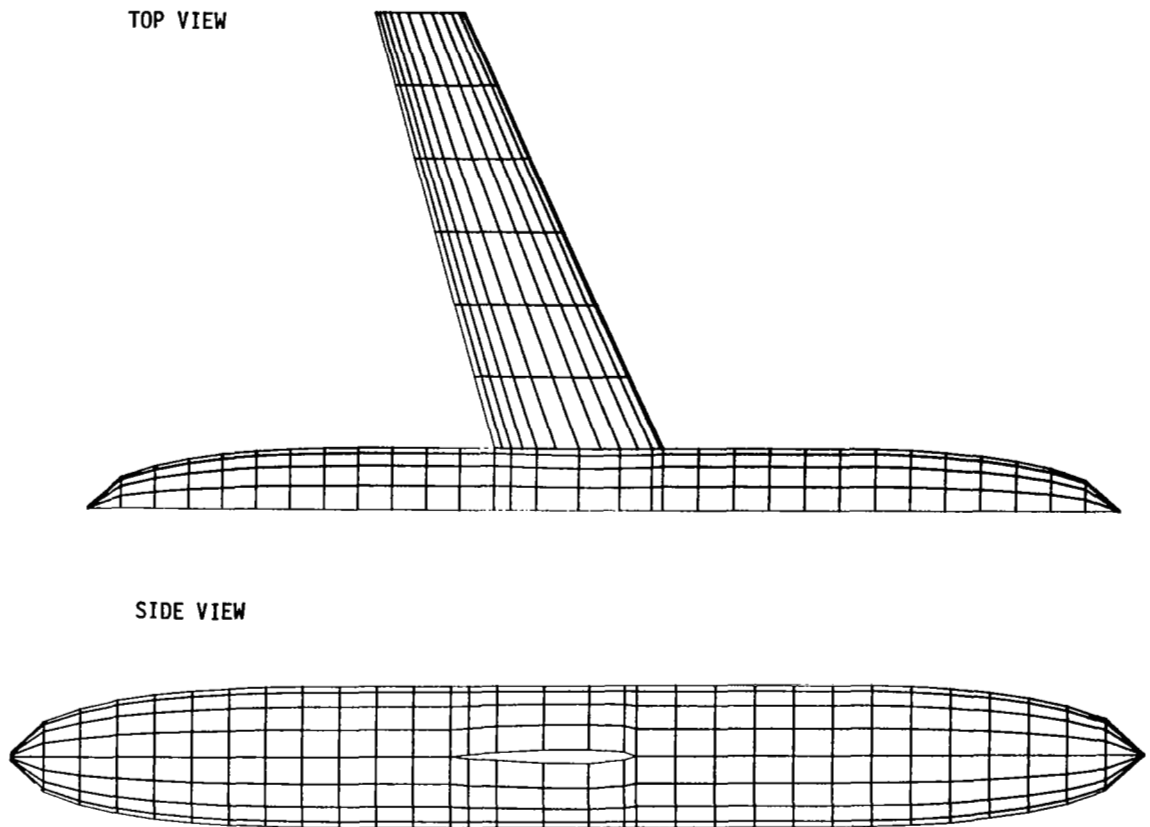


Figure 26. Final repaneling of nonlifting intersection components – wing-fuselage case (zero-incidence wing, N-lines through every other point on intersection curve).

In some cases the intersecting component covers a significant portion of the surface of the intersected component, indicating a need for the use of ignored elements, but the paneling of the intersected component is so coarse that large gaps would be created by their use. The geometry package provides an option which greatly reduces the size of these gaps. In this option a search is conducted to find the points on the intersection curve having the minimum and maximum projected distance in the axial direction on the intersected component from the first point on the first N-line of the component. The intersected component must be paneled using the planar-section mode of operation for this calculation to be performed. The axial direction is defined by the direction cosines of the vector perpendicular to the planes of the N-lines. New N-lines passing through the minimum and maximum points on the intersection curve and lying in planes perpendicular to the

axial direction are then created. The N-lines on either side of the intersection curve are redistributed in a smooth manner using the same procedure as the redistribution of N-lines upstream and downstream of the intersection curve on a non-lifting intersected component. No redistribution of points on the N-lines is performed. The elements covered by the intersecting component are automatically designated as ignored elements by the geometry package and it is possible to proceed directly to the potential-flow solution without checking or changing the results of the geometry package. Figure 27 shows the results of this repaneling option for the wing in a wing-pylon case.

When more accuracy in the region of the intersection curve is desired, a third option can be used, resulting in no gaps between elements. This option first reppanels the intersected component in a manner nearly identical to the one described above. The only difference is that the N-lines immediately on either side of the intersection curve do not actually pass through any of the points on the intersection curve. Instead, each is offset a distance equal to the thickness of the intersecting component (projected in the axial direction). The elements covered by the intersecting component are again designated to be ignored elements. Now the method adds a new nonlifting

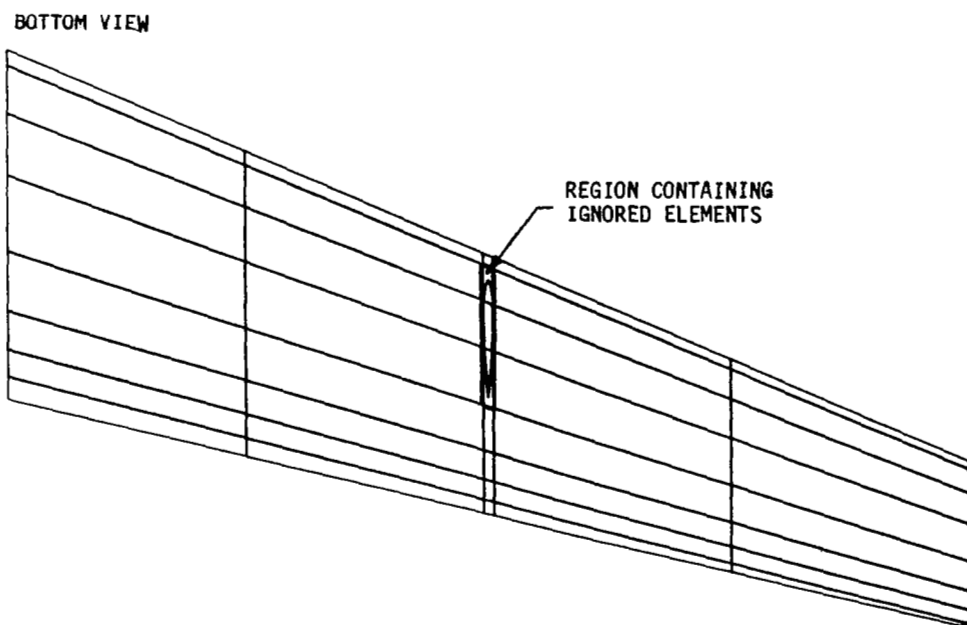


Figure 27. Final repaneling of lifting intersected components — wing-pylon case.



component with elements designed to fill in the gaps around the intersection curve. The new component has only one strip (two N-lines). One of the N-lines coincides with the intersection curve. The other N-line follows the boundaries of the quadrilateral region containing the ignored elements. Figure 28 shows the resulting element distribution for a case with very sparse point spacing on the pylon. Because of the correspondence of the numbers of points on the pylon and on the boundaries of the region containing the ignored elements, the paneling produced only quadrilateral elements (except at the leading and trailing edges of the pylon). If the numbers do not correspond as in figure 28, then one or the other of the N-lines on the new component contains repeated points and triangular elements are produced. Points are repeated in such a way that the length of each M-line on the new component is minimized. Figure 29 shows a case having more points on the pylon than on the boundaries of the region containing the ignored elements, showing the repeated points on one N-line and the resulting triangular elements.

N-lines which bound extra strips falling inside another component are not moved during the repaneling of lifting intersected components. Because of this and because none of the options described above in this section changes the

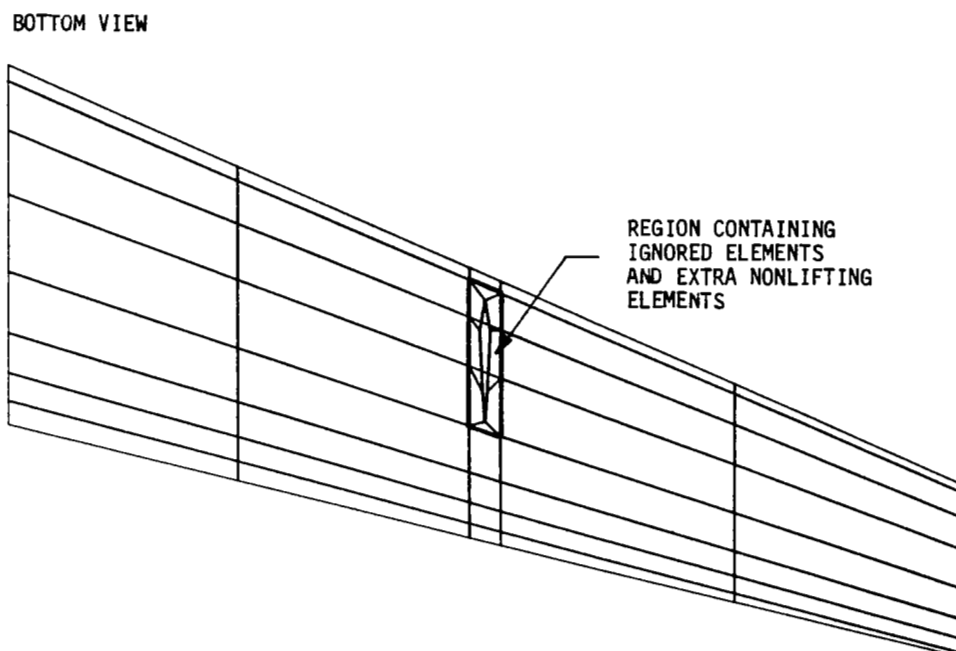


Figure 28. Final repaneling of lifting intersected components — wing-pylon case (sparse element distribution on pylon).

BOTTOM VIEW

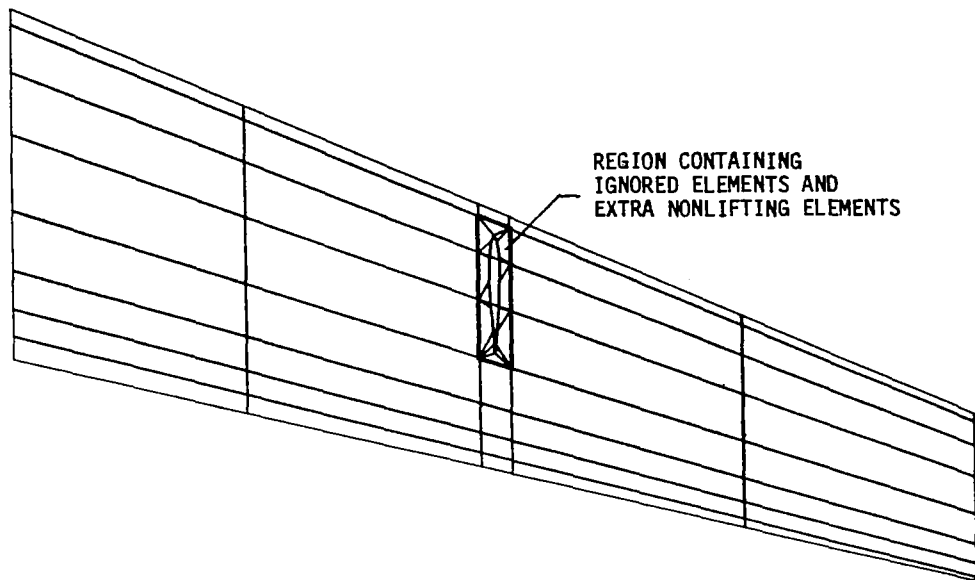


Figure 29. Final repaneling of lifting intersected components — wing-pylon case (more points on pylon than surrounding region on wing).

point distributions on N-lines, the repaneling of a lifting intersected component does nothing to destroy any match-up of the elements along the curve of intersection of the component with another component which it pierces. Therefore, one component can play the role of both an intersected and an intersecting component (although one component cannot intersect or be intersected by more than one other component). Figure 30 shows the final element distribution for a wing-fuselage-pylon case. In this case, the wing and pylon were first repaneled as intersecting components; then the fuselage and the wing were repaneled as intersected components.

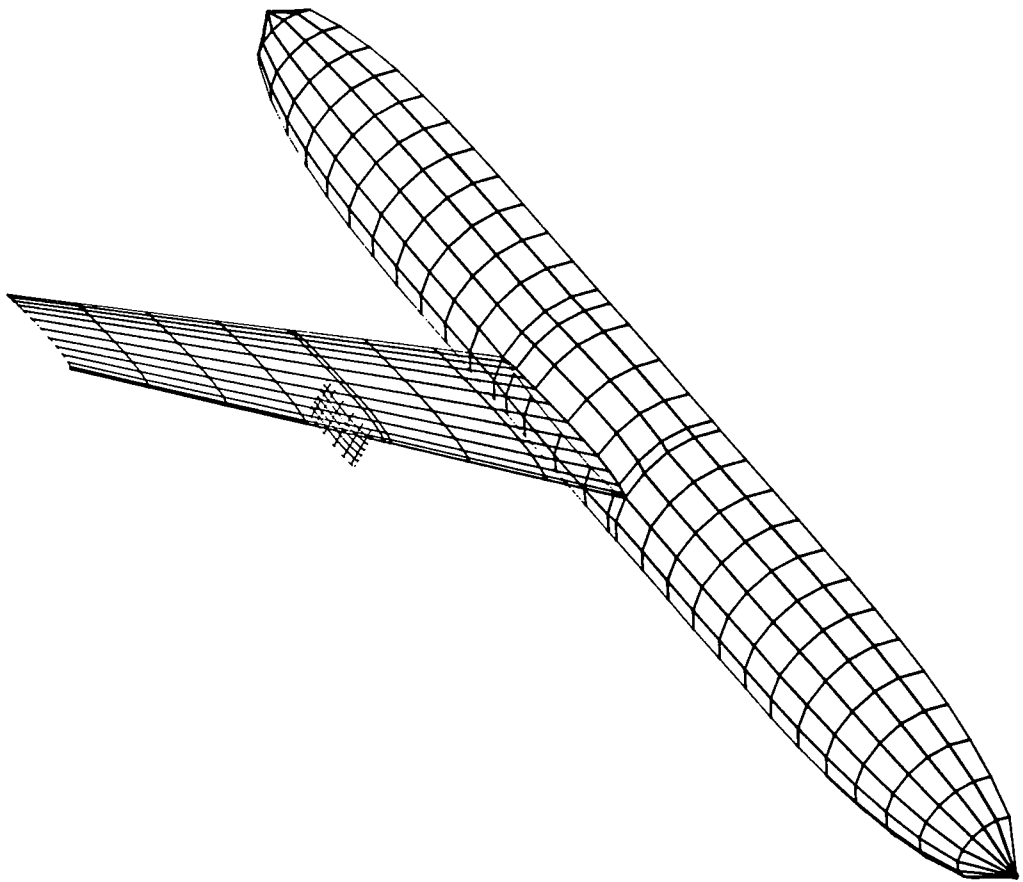


Figure 30. Final element distribution on a wing-fuselage-pylon case.

## 10.0 CONCLUSIONS

The geometry package described above provides a means for significantly reducing the effort required to prepare the input data for three-dimensional potential-flow calculations. Data may be input to the program using either the original input format of reference 4 or the format of reference 5. Geometric input data generally consists of the coordinates of sets of sparsely defined points. In most cases, the number of points input can be at least an order of magnitude less than the number of points required for the potential-flow calculations. Each component of the configuration is automatically paneled using one of several algorithms provided by the method. The number of algorithms provided and the generality of some of them provide the user with a great deal of flexibility in determining the character of the resulting element distributions. Curves of intersection of components are automatically calculated and all intersecting components are rep paneled in a suitable manner for the potential-flow calculations. In many cases the potential-flow calculations can be performed in the same computer run as the geometry package calculations, without interruption. To allow for intermediate checking, however, and to provide for those cases which cannot be run completely without interruption, provision has been made for the punched output of the defining coordinate data at each stage of the geometry calculation in a format suitable for reinput to the program.

## 11.0 REFERENCES

1. Hess, J.L.: Calculation of Potential Flow about Arbitrary Three-Dimensional Lifting Bodies. Final Tech. Rept. McDonnell Douglas Report No. MDC J5679-01, October 1972. (Available from DDC as AD 755 480.)
2. Hess, J.L.: The Problem of Three-Dimensional Lifting Potential Flow and Its Solution by Means of Surface Singularity Distribution. Computer Methods in Applied Mechanics and Engineering, Vol. 4, No. 3, November 1974.
3. Loeve, W. and Sloof, J.W.: On the Use of "Panel Methods" for Predicting Subsonic Flow About Aerofoils and Aircraft Configurations. NLR MP71018U, October 1971.
4. Mack, D.P.: Calculation of Potential Flow about Arbitrary Three-Dimensional Lifting Bodies. Users Manual. McDonnell Douglas Report No. MDC J5679-02, October 1972.
5. Tulinus, J., et al.: Theoretical Prediction of Airplane Stability Derivatives at Subcritical Speeds. NASA CR-132681, 1975.
6. Greville, T.N.E.: Theory and Applications of Spline Functions. Academic Press, New York, 1969.
7. Weber, J.: The Calculation of the Pressure Distribution Over the Surface of Two-Dimensional and Swept Wings with Symmetrical Aerofoil Sections. A.R.C. Tech. Report R&M No. 2918, 1956.
8. Coons, S.A.: Surfaces for Computer-Aided Design of Space Figures. Massachusetts Institute of Technology, ESL Memorandum 9442-M-139, January 1964.
9. Peters, G.J.: Interactive Computer Graphics Application of the Bi-Cubic Parametric Surface to Engineering Design Problems. Paper presented to 1973 National Meeting, Society of Industrial and Applied Mathematics, June 1973.
10. Hess, J.L.: Review of Integral-Equation Techniques for Solving Potential-Flow Problems with Emphasis on the Surface-Source Method. Computer Methods in Applied Mechanics and Engineering, Vol. 5, July 1974.

1. Report No. NASA CR-2962		2. Government Accession No.		3. Recipient's Catalog No.	
4. Title and Subtitle A Geometry Package for Generation of Input Data for a Three-Dimensional Potential-Flow Program				5. Report Date June 1978	
				6. Performing Organization Code	
7. Author(s) N. Douglas Halsey and John L. Hess				8. Performing Organization Report No. MDC J77T0	
9. Performing Organization Name and Address McDonnell Douglas Corporation Douglas Aircraft Company 3855 Lakewood Blvd., Long Beach, Ca. 90846				10. Work Unit No.	
				11. Contract or Grant No. NAS1-14402	
12. Sponsoring Agency Name and Address NASA Langley Research Center Hampton, Va. 23665				13. Type of Report and Period Covered Contractor Report 5/7/76 - 8/22/77	
				14. Sponsoring Agency Code	
15. Supplementary Notes Langley Technical Monitor: James L. Thomas Final Report					
16. Abstract The preparation of geometric data for input to three-dimensional potential-flow programs is a very tedious, time-consuming (and therefore expensive) task. This report describes a geometry package that automates and simplifies this task to a large degree. Input to the computer program for the geometry package consists of a very sparse set of coordinate data, often with an order of magnitude fewer points than required for the actual potential flow calculations. Isolated components, such as wings, fuselages, etc. are paneled automatically, using one of several possible element distribution algorithms. Curves of intersection between components are calculated, using a hybrid curve-fit/surface-fit approach. Finally, intersecting components are rep paneled so that adjacent elements on either side of the intersection curves line up in a satisfactory manner for the potential-flow calculations. The geometry package has been incorporated into the NASA Langley version of the 3-D lifting potential flow program and it is possible to run many cases completely (from input, through the geometry package, and through the flow calculations) without interruption. Use of this geometry package can significantly reduce the time and expense involved in making three-dimensional potential-flow calculations.					
17. Key Words (Suggested by Author(s))  Aerodynamics Geometry Preparation Three-Dimensional Flow			18. Distribution Statement  APPROVED FOR PUBLIC RELEASE; DISTRIBUTION UNLIMITED  Subject Category 02		
19. Security Classif. (of this report) Unclassified		20. Security Classif. (of this page) Unclassified		21. No. of Pages 66	
				22. Price* \$5.25	